

1 Unforeseen plant phenotypic diversity in a dry and grazed world

2 Nicolas Gross^{1,*}, Fernando T. Maestre², Pierre Liancourt^{3,4}, Miguel Berdugo^{5,6}, Raphaël
3 Martin¹, Beatriz Gozalo⁷, Victoria Ochoa⁷, Manuel Delgado-Baquerizo⁸, Vincent Maire⁹, Hugo
4 Saiz¹⁰, Santiago Soliveres^{7,11}, Enrique Valencia⁵, David J. Eldridge¹², Emilio Guirado⁷, Franck
5 Jabot¹, Sergio Asensio⁷, Juan J. Gaitán^{13,14,15}, Miguel García-Gómez¹⁶, Paloma Martínez¹⁷,
6 Jaime Martínez-Valderrama⁷, Betty J. Mendoza¹⁸, Eduardo Moreno-Jiménez¹⁹, David S.
7 Pescador^{18,20}, César Plaza¹⁷, Ivan Santaolara Pijuan⁷, Mehdi Abedi²¹, Rodrigo J. Ahumada²²,
8 Fateh Amghar²³, Antonio I. Arroyo²⁴, Khadijeh Bahalkeh²¹, Lydia Bailey²⁵, Farah Ben Salem²⁶,
9 Niels Blaum²⁷, Bazartseren Boldgiv²⁸, Matthew A. Bowker^{25,29}, Cristina Branquinho³⁰,
10 Liesbeth van den Brink^{4,31}, Chongfeng Bu^{32,33}, Rafaella Canessa^{4,34,35}, Andrea Castillo-
11 Monroy³⁶, Helena Castro³⁷, Patricio Castro³⁸, Roukaya Chibani³⁹, Abel Augusto Conceição⁴⁰,
12 Anthony Darrouzet-Nardi⁴¹, Yvonne C. Davila⁴², Balázs Deák⁴³, David A. Donoso Vargas³⁶,
13 Jorge Durán⁴⁴, Carlos Espinosa⁴⁵, Alex Fajardo^{46,47,48}, Mohammad Farzam⁴⁹, Daniela
14 Ferrante^{50,51}, Jorgelina Franzese⁵², Lauchlan Fraser⁵³, Sofía Gonzalez⁵², Elizabeth Gusman-
15 Montalvan⁴⁵, Rosa Mary Hernández-Hernández⁵⁴, Norbert Hölzel⁵⁵, Elisabeth Huber-
16 Sannwald⁵⁶, Oswaldo Jadan³⁸, Florian Jeltsch²⁷, Anke Jentsch⁵⁷, Mengchen Ju^{32,33}, Kudzai F.
17 Kaseke⁵⁸, Liana Kindermann⁵⁹, Peter le Roux⁶⁰, Anja Linstädter^{59,61}, Michelle A. Louw⁶⁰,
18 Mancha Mabaso⁶², Gillian Maggs-Kölling⁶³, Thulani P. Makhalanyane⁶⁴, Oumarou Malam
19 Issa⁶⁵, Antonio J. Manzaneda⁶⁶, Eugene Marais⁶³, Pierre Margerie⁶⁷, Frederic Mendes
20 Hughes^{40,68,69}, João Vitor S. Messeder⁷⁰, Juan P. Mora⁴⁶, Gerardo Moreno⁷¹, Seth M. Munson⁷²,
21 Alice Nunes³⁰, Gabriel Oliva^{50,51}, Gaston R. Oñatibia⁷³, Guadalupe Peter^{15,74}, Yolanda Pueyo²⁴,
22 R. Emiliano Quiroga^{22,75}, Elizabeth Ramírez-Iglesias⁷⁶, Sasha C. Reed⁷⁷, Pedro J. Rey⁷⁸, Víctor
23 M. Reyes Gómez⁷⁹, Alexandra Rodríguez⁴⁴, Victor Rolo⁷¹, Juan G. Rubalcaba⁵, Jan C.
24 Ruppert⁴, Osvaldo Sala⁸⁰, Ayman Salah⁸¹, Phokgedi Julius Sebei⁸², Ilan Stavi⁸³, Colton
25 Stephens⁵³, Alberto L. Teixido⁵, Andrew D. Thomas⁸⁴, Heather L. Throop^{85,86}, Katja
26 Tielbörger⁴, Samantha Travers⁸⁷, Sainbileg Undrakhbold²⁸, James Val⁸⁷, Orsolya Valkó⁴³,
27 Frederike Velbert⁵⁵, Wanyoike Wamiti⁸⁸, Lixin Wang⁸⁹, Deli Wang⁹⁰, Glenda M. Wardle⁹¹,
28 Peter Wolff⁵⁷, Laura Yahdjian⁷³, Reza Yari⁹², Eli Zaady⁹³, Juan Manuel Zeberio⁷⁴, Yuanling
29 Zhang⁹⁴, Xiaobing Zhou⁹⁴, Yoann Le Bagousse-Pinguet⁹⁵

30

31 *Corresponding author: nicolas.gross@inrae.fr

32 **Author's affiliations**

33 ¹ Université Clermont Auvergne, INRAE, VetAgro Sup, Unité Mixte de Recherche Ecosystème
34 Prairial; Clermont-Ferrand, France

35 ² Environmental Sciences and Engineering, Biological and Environmental Science and
36 Engineering Division, King Abdullah University of Science and Technology, Thuwal, 23955-
37 6900, Kingdom of Saudi Arabia

38 ³ Institute Botany Department. State Museum of Natural History Stuttgart; Stuttgart, Germany

39 ⁴ Plant Ecology Group, University of Tübingen, Tübingen, Germany

40 ⁵ Departamento de Biodiversidad, Ecología y Evolución, Facultad de Ciencias Biológicas,
41 Universidad Complutense de Madrid, 28040, Madrid, Spain

42 ⁶ Department of Environmental Systems Science, ETH Zurich; Zurich, Switzerland

43 ⁷ Instituto Multidisciplinar para el Estudio del Medio “Ramon Margalef”, Universidad de
44 Alicante, Alicante, Spain

45 ⁸ Laboratorio de Biodiversidad y Funcionamiento Ecosistémico. Instituto de Recursos Naturales
46 y Agrobiología de Sevilla (IRNAS), CSIC; Sevilla, Spain

47 ⁹ Département des sciences de l'environnement, Université du Québec à Trois-Rivières, Trois
48 Rivières, Canada

49 ¹⁰ Departamento de Ciencias Agrarias y Medio Natural, Escuela Politécnica Superior, Instituto
50 Universitario de Investigación en Ciencias Ambientales de Aragón (IUCA), Universidad de
51 Zaragoza, Huesca, Spain

52 ¹¹ Departamento de Ecología, Universidad de Alicante, Alicante, Spain

53 ¹² Centre for Ecosystem Science, School of Biological, Earth and Environmental Sciences,
54 University of New South Wales; Sydney, Australia

55 ¹³ Instituto Nacional de Tecnología Agropecuaria (INTA), Instituto de Suelos-CNIA; Buenos
56 Aires, Argentina

57 ¹⁴ Universidad Nacional de Luján, Departamento de Tecnología; Luján, Argentina

58 ¹⁵ Consejo Nacional de Investigaciones Científicas y Técnicas de Argentina (CONICET);
59 Buenos Aires, Argentina

60 ¹⁶ Departamento de Ingeniería y Morfología del Terreno, Escuela Técnica Superior de
61 Ingenieros de Caminos, Canales y Puertos, Universidad Politécnica de Madrid; Madrid, Spain

62 ¹⁷ Instituto de Ciencias Agrarias, Consejo Superior de Investigaciones Científicas; Madrid,
63 Spain

64 ¹⁸ Departamento de Biología y Geología, Física y Química Inorgánica, Universidad Rey Juan
65 Carlos; Móstoles, Spain

66 ¹⁹ Department of Agricultural and Food Chemistry, Faculty of Sciences, Universidad Autónoma
67 de Madrid; Madrid, Spain.

68 ²⁰ Departamento de Farmacología, Farmacognosia y Botánica, Facultad de Farmacia,
69 Universidad Complutense de Madrid; Madrid, Spain

70 ²¹ Department of Range Management, Faculty of Natural Resources and Marine Sciences,
71 Tarbiat Modares University; Noor, Mazandaran Province, I. R. Iran

72 ²² Instituto Nacional de Tecnología Agropecuaria, Estación Experimental Agropecuaria
73 Catamarca, Catamarca, Argentina

74 ²³ Laboratoire de Recherche: Biodiversité, Biotechnologie, Environnement et Développement
75 Durable (BioDev), Faculté des Sciences, Université M'hamed Bougara de Boumerdès;
76 Boumerdès, Algérie

77 ²⁴ Instituto Pirenaico de Ecología (IPE, CSIC) Montañana Avenue 1005, 50159, Zaragoza,
78 Spain

79 ²⁵ Center for Ecosystem Science and Society, Northern Arizona University, Flagstaff, AZ, USA

80 ²⁶ Laboratory of pastoral ecosystems and promotion of spontaneous plants and associated
81 micro-organisms, Institut des Régions Arides (IRA) Médenine, University of Gabes, Tunisia

82 ²⁷ University of Potsdam, Plant Ecology & Nature Conservation, Am Mühlenberg 3, 14476
83 Potsdam

84 ²⁸ Department of Biology, School of Arts and Sciences, National University of Mongolia,
85 Ulaanbaatar 14201, Mongolia

86 ²⁹ School of Forestry, Northern Arizona University, Flagstaff, AZ, USA.

87 ³⁰ cE3c - Centre for Ecology, Evolution and Environmental Changes & CHANGE – Global
88 Change and Sustainability Institute, Faculdade de Ciências, Universidade de Lisboa, 1749-016
89 Lisboa, Portugal

90 ³¹ ECOBIOSIS, Departamento of Botánica, Universidad de Concepción, Chile

91 ³² Institute of Soil and Water Conservation, Northwest A & F University; Yangling, Shaanxi,
92 China

93 ³³ Institute of Soil and Water Conservation, Chinese Academy of Sciences and Ministry of
94 Water Resources; Yangling, Shaanxi, China

95 ³⁴ German Centre for Integrative Biodiversity Research (iDiv) Halle-Jena-Leipzig, Puschstrasse
96 4, 04103 Leipzig, Germany

97 ³⁵ Institut für Biologie, Martin-Luther-University Halle-Wittenberg, Halle, Germany

98 ³⁶ Departamento de Biología, Escuela Politécnica Nacional, Quito, Ecuador

99 ³⁷ University of Coimbra, Centre for Functional Ecology, Department of Life Sciences;
100 Coimbra, Portugal

101 ³⁸ Universidad de Cuenca, Facultad de Ciencias Agropecuarias, Carrera de Ingeniería
102 Agronómica, Grupo de Agroforestería, Manejo y Conservación del paisaje, Cuenca, Ecuador

103 ³⁹ Laboratory of Eremology and combating desertification, Institut des Régions Arides (IRA)
104 Médenine, University of Gabes, Tunisia

105 ⁴⁰ Departamento de Ciências Biológicas da Universidade Estadual de Feira de Santana, Bahia,
106 Brasil

107 ⁴¹ Department of Biological Sciences, University of Texas at El Paso; El Paso, TX, USA.

108 ⁴² Faculty of Science, University of Technology Sydney, Sydney New South Wales 2007,
109 Australia

110 ⁴³ Lendület' Seed Ecology Research Group, Institute of Ecology and Botany, Centre for
111 Ecological Research, 2-4 Alkotmány street, H-2163 Vácrátót, Hungary

112 ⁴⁴ Misión Biológica de Galicia, CSIC; Pontevedra, Spain

113 ⁴⁵ Departamento de Ciencias Biológicas y Agropecuarias. Universidad Técnica Particular de
114 Loja, Ecuador

115 ⁴⁶ Instituto de Investigación Interdisciplinaria (I3), Vicerrectoría Académica, Universidad de
116 Talca, Chile

117 ⁴⁷ Instituto de Ecología y Biodiversidad (IEB), Las Palmeras 3425, Santiago, Chile

118 ⁴⁸ Instituto Milenio, Limits of Life (LiLi), Valdivia, Chile

119 ⁴⁹ Department of Range and Watershed Management, Faculty of Natural Resources and
120 Environment, Ferdowsi University of Mashhad, Mashhad, Iran.

121 ⁵⁰ Instituto Nacional de Tecnología Agropecuaria EEA Santa Cruz; Río Gallegos, Santa Cruz,
122 Argentina

123 ⁵¹ Universidad Nacional de la Patagonia Austral; Río Gallegos, Santa Cruz, Argentina

124 ⁵² Instituto de Investigaciones en Biodiversidad y Medioambiente (Consejo Nacional de
125 Investigaciones Científicas y Técnicas-Universidad Nacional del Comahue), Argentina

126 ⁵³ Department of Natural Resource Science, Thompson Rivers University; British Columbia,
127 Canada

128 ⁵⁴ Universidad Nacional Experimental Simón Rodríguez (UNESR), Instituto de Estudios
129 Científicos y Tecnológicos (IDECYT); Centro de Estudios de Agroecología Tropical
130 (CEDAT); Miranda, Venezuela

131 ⁵⁵ Institute of Landscape Ecology, University of Münster; Münster, Germany

132 ⁵⁶ Instituto Potosino de Investigación Científica y Tecnológica, A.C.; San Luis Potosí, México

133 ⁵⁷ Department of Disturbance Ecology, Bayreuth Center of Ecology and Environmental
134 Research BayCEER, University of Bayreuth; Bayreuth, Germany

135 ⁵⁸ Kudzai F. Kaseke, Earth Research Institute, University of California Santa Barbara, CA
136 93106, USA

137 ⁵⁹ Biodiversity Research/ Systematic Botany Group, Institute of Biochemistry and Biology,
138 University of Potsdam; Potsdam, Germany

139 ⁶⁰ Department of Plant and Soil Sciences, University of Pretoria; Pretoria, South Africa

140 ⁶¹ Institute of Crop Science and Resource Conservation, University of Bonn; Bonn, Germany

141 ⁶² Department of Biochemistry, Genetics and Microbiology, DSI/NRF SARChI in Marine
142 Microbiomics, University of Pretoria, Hatfield, Lynnwood Road, Pretoria, South Africa

143 ⁶³ Gobabeb-Namib Research Institute, Walvis Bay, Namibia

144 ⁶⁴ Department of Microbiology, Faculty of Science, Stellenbosch University, Stellenbosch,
145 South Africa.

146 ⁶⁵ Institut d'Écologie et des Sciences de l'Environnement de Paris (iEES-Paris), Sorbonne
147 Université, IRD, CNRS, INRAE, Université Paris Est Creteil, Université de Paris, Centre IRD
148 de France Nord; Bondy, France

149 ⁶⁶ Dept. Biología Animal, Biología Vegetal y Ecología. Universidad de Jaén

150 ⁶⁷ Normandie Univ, UNIROUEN, INRAE, ECODIV, 76000 Rouen, France.

151 ⁶⁸ Programa de Pós-graduação em Zoologia and Conselho de Curadores das Coleções
152 Científicas, Universidade Estadual de Santa Cruz, Rodovia Jorge Amado, 45662-900, Ilhéus,
153 Bahia, Brazil

154 ⁶⁹ Programa de Pós-graduação em Bioinformática, Universidade Federal de Minas Gerais, Av.
155 Antônio Carlos, 31270-901, Pampulha, Belo Horizonte, MG, Brazil

156 ⁷⁰ Biology Department & Ecology Program, The Pennsylvania State University, University
157 Park, Pennsylvania, USA - 16802

158 ⁷¹ Forestry School, INDEHESA, Universidad de Extremadura, Plasencia, Spain

159 ⁷² U.S. Geological Survey, Southwest Biological Science Center, Flagstaff, AZ 86001 USA

160 ⁷³ Cátedra de Ecología, Facultad de Agronomía, Universidad de Buenos Aires. Instituto de
161 Investigaciones Fisiológicas y Ecológicas Vinculadas a la Agricultura (IFEVA-CONICET);
162 Ciudad Autónoma de Buenos Aires, Argentina

163 ⁷⁴ Universidad Nacional de Río Negro, Sede Atlántica, CEANPa; Río Negro, Argentina

164 ⁷⁵ Cátedra de Manejo de Pastizales Naturales, Facultad de Ciencias Agrarias, Universidad
165 Nacional de Catamarca, Catamarca, Argentina

166 ⁷⁶ Universidad Estatal Amazónica (UEA), Puyo-Ecuador

167 ⁷⁷ US Geological Survey, Southwest Biological Science Center; Moab, UT, USA

168 ⁷⁸ Instituto Interuniversitario de Investigación del Sistema Tierra de Andalucía. Universidad de
169 Jaén

170 ⁷⁹ Institute of Ecology A.C. Environment and Sustainability Network, Chihuahua

171 ⁸⁰ Global Drylands Center, School of Life Sciences and School of Sustainability, Arizona State
172 University

173 ⁸¹ Al Quds University; Palestine

174 ⁸² Mara Research Station, Limpopo Department of Agriculture and Rural Development, South
175 Africa

176 ⁸³ Dead Sea and Arava Science Center, Yotvata, Israel

177 ⁸⁴ Department of Geography and Earth Sciences, Aberystwyth University, Wales, UK

178 ⁸⁵ School of Earth and Space Exploration, Arizona State University, Tempe, AZ, USA

179 ⁸⁶ School of Life Sciences, Arizona State University, Tempe, AZ, USA

180 ⁸⁷ Department of Planning and Environment, c/o Centre for Ecosystem Science, School of
181 Biological, Earth and Environmental Sciences, University of New South Wales; Sydney,
182 Australia

183 ⁸⁸ Zoology Department, National Museums of Kenya, P.O. Box 40658-00100; Nairobi, Kenya

184 ⁸⁹ Department of Earth Sciences, Indiana University Indianapolis (IUI), Indianapolis, Indiana
185 46202, USA

186 ⁹⁰ Key Laboratory of Vegetation Ecology of the Ministry of Education, Jilin Songnen Grassland
187 Ecosystem National Observation and Research Station, Institute of Grassland Science,
188 Northeast Normal University; Changchun, China

189 ⁹¹ Desert Ecology Research Group, School of Life and Environmental Sciences, The University
190 of Sydney, Sydney, New South Wales 2006, Australia

191 ⁹² Forest and Rangeland Research Department, Khorasan Razavi Agricultural and Natural
192 Resources Research and Education Center. AREEO, Mashhad, Iran.

193 ⁹³ Department of Natural Resources, Agricultural Research Organization, Institute of Plant
194 Sciences, Gilat Research Center; Mobile Post Negev, Israel

195 ⁹⁴ State Key Laboratory of Desert and Oasis Ecology, Key Laboratory of Ecological Safety and
196 Sustainable Development in Arid Lands, Xinjiang Institute of Ecology and Geography,
197 Chinese Academy of Sciences

198 ⁹⁵ Aix Marseille Univ, CNRS, Avignon Université, IRD, IMBE; Aix-en-Provence, France

199 **Earth harbors an extraordinary plant phenotypic diversity¹ that is at risk from ongoing**
200 **global changes^{2,3}. However, we do not know how increasing aridity and livestock grazing**
201 **pressure - two major global change drivers⁴⁻⁶ shape the trait covariation underlying plant**
202 **phenotypic diversity^{1,7}. Here, we assessed how covariation among 20 chemical and**
203 **morphological traits responds to aridity and grazing pressure within global drylands. Our**
204 **analysis involved 133,769 trait measurements spanning 1,347 observations of perennial**
205 **plant species surveyed across 326 plots from six continents. Crossing an aridity threshold**
206 **of ~0.7 (close to the transition between semi-arid and arid zones) led to an unexpected**
207 **88% increase in trait diversity. This threshold appeared in the presence of grazers, and**
208 **moved toward lower aridity levels with increasing grazing pressure. Moreover, 57% of**
209 **observed trait diversity only occurred in the most arid and grazed drylands surveyed,**
210 **highlighting the phenotypic uniqueness of these extreme environments. Our work**
211 **indicates that drylands act as a global reservoir of plant phenotypic diversity and**
212 **challenge the pervasive view that harsh environmental conditions reduce plant trait**
213 **diversity⁸⁻¹⁰. They also highlight that many alternative strategies may allow plants to cope**
214 **with increases in environmental stress induced by climate change and land-use**
215 **intensification.**

216

217 The recent development of global trait databases¹¹ has been instrumental for characterizing the
218 phenotypic diversity (trait diversity hereafter) of the entire plant kingdom^{1,7,12}. This
219 characterization is fundamental to anticipate the effects of global change on biodiversity and
220 the functioning of the biosphere^{2,13}. Yet, our understanding of plant trait diversity has been
221 biased towards mesic biomes^{14,15} (e.g., tropical and temperate regions). Although the
222 geographical coverage of trait observations is currently increasing¹¹, many regions of the globe
223 remain poorly explored^{14,15}. In particular, drylands remain largely underrepresented in global
224 trait databases¹⁵ (Supplementary Table 1) despite the fact that they cover ~45% of the planet's
225 terrestrial area¹⁶, are present over all latitudes and continents¹⁷, and are projected to expand due
226 to climate change and associated increases in aridity¹⁸ (defined as $1 - \text{aridity index}^5$; aridity
227 index = mean annual precipitation \div potential evapotranspiration¹⁹). Drylands are highly
228 vulnerable to multiple global change drivers⁴⁻⁶ including changes in aridity and pressure from
229 livestock grazing, the major land use across drylands⁶. For instance, crossing an aridity
230 threshold of 0.7 or increasing grazing pressure can lead to abrupt and systemic changes in
231 multiple ecosystem attributes^{5,6}, including drastic decreases in plant species richness and cover

232 that may lead to land degradation and desertification²⁰. However, it remains virtually unknown
233 how increasing aridity and grazing pressure jointly shape trait diversity of drylands at a global
234 scale. This knowledge is needed to make reliable predictions of the future of biodiversity^{2,13}
235 and the functioning of dryland ecosystems^{17,21} under global change.

236 One may expect that crossing aridity thresholds and increasing grazing pressure should
237 reduce trait diversity in drylands²² by selecting only those species able to tolerate extreme
238 temperatures, low soil nutrient contents and water availability, and high stocking rates (see the
239 pervasive “environmental filtering” concept^{8–10} and associated hypotheses in Supplementary
240 Text 1 and Supplementary Figure 1). However, drylands can exhibit a startling diversity of
241 plant forms and functions^{22,23} (the so-called “functional paradox of drylands”¹⁷), which
242 seemingly contradicts the environmental filtering concept. This paradox may arise because
243 distinct trait syndromes can perform equally in response to a specific environmental
244 constraint^{24,25}, thus allowing alternative plant strategies to persist in harsh environments
245 (Supplementary Text 1). Given the importance of trait diversity in the provisioning of essential
246 ecosystem services²⁶ to the more than 2 billion people inhabiting dryland areas²⁰, understanding
247 this discrepancy is a crucial research need.

248 Plant traits covary predictably among species because of evolutionary and ecological
249 constraints limiting the number of viable trait combinations^{1,7,12} that ultimately determine the
250 extent of plant trait diversity¹. Global initiatives aiming to characterize the fundamental
251 dimensions of trait covariation have focused mainly on plant morphological diversity^{1,7,12} and
252 leaf carbon economy²⁷, but have largely neglected the diversity of chemical elements that
253 sustain plant survival and growth^{28,29}. The elemental concentration in plant leaves (plant
254 elementome hereafter) has major implications for plant development³⁰, animal and human
255 health^{31,32}, and global biogeochemical cycles²⁸. Furthermore, the plant elementome has a
256 pivotal role in determining plant responses to water scarcity^{33–35} and herbivory^{36,37}
257 (Supplementary Table 2). However, we do not know how the plant elementome is distributed
258 across plant species, and how it contributes to trait diversity patterns across global drylands.
259 Accounting for the plant elementome may thus reveal new functional dimensions with the
260 potential to change our understanding of plant strategies in drylands and their responses to
261 ongoing global changes.

262 Here, we conducted a standardized field survey to investigate the impacts of aridity and
263 grazing pressure on the chemical and morphological trait diversity of perennial plants across
264 drylands worldwide (Figure 1). We selected 98 sites from 25 countries that represent the aridity

265 gradient over which dryland rangelands can be found globally⁶. Each site included three to four
266 45 m × 45 m plots spanning local gradients of grazing pressure (from ungrazed or low grazing
267 pressure to high grazing pressure), with a total of 326 plots surveyed. In each plot, we measured
268 a total of 20 continuous traits related to: i) the concentration of 14 chemical elements in plant
269 leaves (i.e., C, N, P, K, Mg, Ca, S, Zn, Na, Cu, Mn, Fe, Ba, and Al), ii) the leaf and whole plant
270 size (i.e., lateral spread, maximum plant height, leaf length, and leaf area), and iii) the leaf C-
271 economy (i.e., specific leaf area, SLA; and leaf dry matter content, LDMC). Our database
272 included 1,347 observations of dryland plant species sampled across 326 plots from all latitudes
273 and continents (Figure 1) for which the complete set of these 20 traits was measured (total
274 number of traits measurements = 133,769; see Supplementary Table 3 for a full description of
275 the database and Supplementary Figures 2-4 for the frequency distribution of these traits). This
276 database constitutes a unique source of functional information to explore how aridity and
277 grazing shape the covariations and trade-offs observed among multiple morphological and
278 chemical plant traits across global drylands.

279

280 **Aridity and grazing sharply increase trait diversity across global drylands**

281 We used a sliding windows analysis (see Methods) to evaluate changes in dryland trait diversity
282 in response to increases in aridity and grazing pressure. To do so, we ordered the 326 plots
283 surveyed according to their aridity level. We then defined aridity windows that represent 19%
284 of the global aridity gradient considered, and selected all plant species from all plots within this
285 aridity range ($n = 307$ observations in each window). For each aridity window, we quantified
286 the n -dimensional trait space using the plant elementome, and morphological and C-economy
287 related traits (i.e., trait hypervolume³⁸; see Methods and Extended Data Figure 1,
288 Supplementary Figures 5-8, and Supplementary Table 4 for a description of the dryland trait
289 space evaluated). The size of the hypervolume provides a measure of the trait diversity³⁸
290 considered within each aridity window.

291 Increases in aridity were associated with an unforeseen increase in plant trait diversity
292 (dashed line in Fig. 2a; see also Supplementary Table 5). We found a significant threshold
293 response in the trait hypervolume occurring at an aridity value ~ 0.7 (Fig. 2). Aridity values
294 exceeding this threshold were associated with an 88.1 % increase in the size of the trait
295 hypervolume in the driest rangelands surveyed (Fig. 2b; Supplementary Figure 9). The trait
296 hypervolume observed at high aridity levels largely encompassed and surpassed the

297 morphological and chemical trait diversity observed under low aridity conditions: 80.1 % of
298 the low-aridity hypervolume was included within the high-aridity hypervolume and 57.3 % of
299 the global dryland trait diversity was only observed under aridity values higher than ~0.7 (Fig.
300 2b). We also observed an increase of the size of the trait hypervolume with increasing grazing
301 pressure (Fig. 2c). Aridity and grazing thus have a similar effect on trait diversity by promoting
302 a wide spectrum of plant strategies to cope with water shortage^{17,23,25} and herbivory^{39,40} through
303 a variety of avoidance and tolerance strategies. Our results support theoretical predictions²⁴ and
304 empirical observations from drylands^{17,22,23} and other extreme environments (e.g., alpine
305 ecosystems⁴¹), which suggest that there are many ways for species to cope with climatic
306 extremes and grazing pressure. The most arid dryland rangelands thus harbor a unique trait
307 diversity, highlighting their importance as a global reservoir of plant form and function and
308 reinforcing the biological and evolutionary importance of dryland ecosystems.

309

310 **The elementome is key to explain trait diversity responses to global change drivers**

311 The sharp increase in trait diversity observed with increases in aridity and grazing pressure
312 resulted mainly from a decrease in trait covariation at aridity values higher than ~0.7 (Fig. 3).
313 Specifically, both aridity (Extended Data Figure 2; Supplementary Table 4) and the presence
314 of grazers (Extended Data Figure 3; Supplementary Table 6) increased the number of trait
315 dimensions within the dryland plant trait spectrum, resulting in the presence of extreme
316 phenotypes exhibiting unique trait syndromes in the driest rangelands surveyed. For instance,
317 all macronutrients correlated along a unique principal component (PC) axis below the ~0.7
318 aridity threshold (PC1 in Extended Data Figure 2a, b). After exceeding the ~0.7 aridity
319 threshold, primary and secondary macronutrients - namely N-P-K and Mg-Ca-S - became
320 independent and segregated along two different axes (Extended Data Figure 2c, d, e),
321 highlighting a decoupling between macronutrients in plants under high aridity conditions.

322 High aridity levels also promoted functionally contrasting strategies (see Extended Data
323 Figure 4), such as tall species with fast growing leaves following stress-avoidance strategies^{22,25}
324 (defined by high N-P-K and low LDMC values) and small conservative species following
325 stress-tolerance strategies^{1,42} (defined by low N-P-K and high LDMC values; Extended Data
326 Figure 4b) with either low or high Mg-Ca (Extended Data Figure 4a), and Zn-Na (Extended
327 Data Figure 4c) concentrations in leaves. These elemental strategies can reflect the contrasting
328 role of chemical elements in plants, either as a way to tolerate high aridity levels³³⁻³⁵, or as base

329 elements for defensive compounds against herbivory^{36,37,43} (Supplementary Table 2). By
330 identifying an abrupt change in trait variations among plant chemical elements occurring at
331 aridity values ~ 0.7 , our findings highlight the importance of considering the plant elementome
332 to accurately grasp dryland biodiversity responses to ongoing climate change.

333

334 **Biotic processes and global change-driven biodiversity patterns**

335 The abrupt increase in trait diversity with aridity observed corresponds with one of the recently
336 identified ecosystem thresholds operating on drylands worldwide⁵, which is characterized by
337 declines in soil fertility and plant cover after an aridity value of ~ 0.7 is crossed. The
338 simultaneous occurrence of alterations in crucial aspects of drylands and trait diversity presents
339 a distinctive opportunity to uncover the underlying mechanisms through which increasing
340 aridity and grazing pressure impact on dryland ecosystems.

341 We first hypothesized that abrupt declines in soil fertility could explain the changes in
342 plant trait diversity observed once the aridity threshold of ~ 0.7 is crossed. This is attributed to
343 the fact that variations in the chemical diversity of soils (the soil elementome) across different
344 sites can directly affect the plant elementome^{29,44}. We tested this hypothesis by measuring the
345 soil elemental concentration of the 326 plots surveyed (see Methods; and Extended Data Figure
346 5). Contrary to what is observed across plant leaves (Extended Data Figure 1; Supplementary
347 Figure 5), we found a strong covariation within the soil elementome (Extended Data Figure 5a,
348 b; Supplementary Figure 10). All soil elements aligned along a unique principal component that
349 accounts for 65.8% of the total variation observed in the soil elementome, a pattern that further
350 increased in the most arid areas (Extended Data Figure 5c; Supplementary Table 7). These
351 results did not support our hypothesis. Rather, they suggest a strong decoupling between the
352 soil and plant elementome, and therefore that plant elemental concentration reflects
353 independent dimensions through which dryland plant species segregate across contrasting
354 functional strategies²⁹.

355 Alternatively, we hypothesized that declines in plant cover may explain the observed
356 pattern of increased trait diversity with aridity. Since the decline in plant cover can alter
357 interactions among plants (e.g., release of competitive interactions and collapse of positive
358 interactions – incl. facilitation and plant-soil feedback^{5,42,45}), we expected that increasing aridity
359 would promote the persistence of competitively weak, but well-adapted phenotypes to aridity
360 (see Supplementary Text 2 and Supplementary Figures 11, 12 for a rationale for this

361 hypothesis). To test this hypothesis, we measured *in situ* total plant cover across all of our sites
362 (see Methods) and found that it was sharply reduced below ~ 50% after crossing the ~0.7 aridity
363 threshold (Extended Data Figure 6). We substituted aridity with plant cover in our sliding
364 windows procedure, and showed that crossing a ~ 50% value in plant cover was associated with
365 both an increase in the trait hypervolume and a decrease in trait covariation (Extended Data
366 Figure 7; Supplementary Table 8). At cover values higher than 50%, large vegetation patches
367 may emerge from spatial constraints only (see the so-called spanning clusters in percolation
368 theory^{46–48}) forcing plant individuals to compete for space. In contrast, the decrease in plant
369 cover below 50% may release competitive interactions as plant individuals would have space
370 to thrive by avoiding competitive interactions^{42,45}. The match between the ~0.7 aridity threshold
371 and the 50% threshold in plant cover therefore reinforces our hypothesis that the observed
372 pattern of increase in trait diversity with aridity may be driven by a collapse of plant-plant
373 interactions^{5,45}. Our results challenge the pervasive environmental filtering concept^{8–10}, which
374 posits that the abiotic environment should select for a narrow set of trait values and reduce trait
375 diversity in the most severe environments. In contrast, they revealed that increasing plant cover
376 and the associated biotic processes^{42,45} act as a global filter of plant biodiversity thereby
377 reducing plant phenotypic diversity by half in the most productive compared to the most arid
378 dryland areas.

379 Grazing was a main driver of decreasing plant cover (Extended Data Figure 6a, c) and
380 significantly modulated both the shape and location of the aridity threshold (Fig. 4; and
381 Supplementary Table 9), indicating that climate and land use changes interact to determine
382 phenotypic plant diversity. Specifically, the absence of grazing shifted the observed aridity
383 threshold for trait covariation towards a higher aridity value compared to other grazing pressure
384 levels (Fig. 4). Furthermore, removing grazing smoothed aridity impacts on trait hypervolume,
385 leading to a weak linear response of trait diversity to aridity observed in absence of grazers
386 (Fig. 4). Altogether, our results also show that by modifying plant cover, grazing pressure can
387 modulate the response of trait diversity to increasing aridity, and thus alter the trait space of
388 dryland plant species worldwide.

389 Our results shed new light on the dryland functional paradox¹⁷ by identifying a “plant
390 loneliness syndrome”, where the scattered plants across the most arid rangeland landscapes in
391 drylands exhibit high degree of trait uniqueness. This syndrome may directly result from the
392 collapse of biotic interactions associated with the low plant cover occurring in these
393 environments^{45,48}, and from the large spatio-temporal variation in the distribution of limiting

394 resources⁴⁹. Regardless of the mechanisms involved, the “plant loneliness syndrome” promotes
395 a strikingly high plant trait diversity at the dry edge of perennial plant life. Combined with the
396 general decline in plant taxonomic richness observed in the most arid drylands⁵, our results
397 highlight a very low functional redundancy in the species pool of the dryland plant flora, which
398 could compromise their resistance and resilience to further disturbances⁵⁰.

399

400 **Conclusion**

401 We identified an abrupt reorganization of the dryland trait space after crossing an aridity value
402 of ~0.7. Once this threshold was reached, small increases in aridity led to an abrupt increase of
403 trait diversity. These changes were linked to a decoupling in the plant elementome. Similarly,
404 increases in grazing pressure substantially increased trait diversity and modulated the aridity
405 threshold identified. Our findings illustrate how climate and land use interact to shape
406 phenotypic plant diversity in drylands, and bring both empirical and mechanistic evidence to
407 the “dryland functional paradox”¹⁷. They question the predictions of the pervasive
408 environmental filtering concept⁸⁻¹⁰ that single trait optima allow species to persist in new
409 environments. Our study also delivers novel insights into how vascular plants respond to biotic
410 stressors and environmental extremes, and shed light on how the global plant functional trait
411 space may be shaped by joint increases in aridity and grazing pressure, which are becoming
412 more common in a drier and human-dominated world. Finally, our data and results can help to
413 better understand the provisioning of essential nutrients to livestock and human populations in
414 drylands under ongoing global environmental change.

415

416

417

418

419

420

421

422

423

424 **References (Main Text)**

- 425 1. Díaz, S. *et al.* The global spectrum of plant form and function. *Nature* **529**, 167–171 (2016).
- 426 2. IPBES. *Summary for Policymakers of the Global Assessment Report on Biodiversity and*
427 *Ecosystem Services*. (2019) doi:10.5281/zenodo.3553579.
- 428 3. Carmona, C. P. *et al.* Erosion of global functional diversity across the tree of life. *Sci. Adv.*
429 **7**, eabf2675 (2021).
- 430 4. Shukla, P. R. *et al.* Climate Change and Land: an IPCC special report on climate change,
431 desertification, land degradation, sustainable land management, food security, and
432 greenhouse gas fluxes in terrestrial ecosystems. (2019).
- 433 5. Berdugo, M. *et al.* Global ecosystem thresholds driven by aridity. *Science* **367**, 787–790
434 (2020).
- 435 6. Maestre, F. T. *et al.* Grazing and ecosystem service delivery in global drylands. *Science*
436 **378**, 915–920 (2022).
- 437 7. Joswig, J. S. *et al.* Climatic and soil factors explain the two-dimensional spectrum of global
438 plant trait variation. *Nature Ecology & Evolution* **6**, 36–50 (2022).
- 439 8. Keddy, P. A. Assembly and response rules: two goals for predictive community ecology. *J*
440 *Vegetation Science* **3**, 157–164 (1992).
- 441 9. Kraft, N. J. B. *et al.* Community assembly, coexistence and the environmental filtering
442 metaphor. *Functional Ecology* **29**, 592–599 (2015).
- 443 10. Enquist, B. J. *et al.* Scaling from traits to ecosystems: developing a general trait driver
444 theory via integrating trait-based and metabolic scaling theories. in *Advances in ecological*
445 *research* vol. 52 249–318 (Elsevier, 2015).
- 446 11. Kattge, J. *et al.* TRY plant trait database – enhanced coverage and open access. *Global*
447 *Change Biology* **26**, 119–188 (2020).
- 448 12. Carmona, C. P. *et al.* Fine-root traits in the global spectrum of plant form and function.
449 *Nature* **597**, 683–687 (2021).
- 450 13. Urban, M. C. *et al.* Improving the forecast for biodiversity under climate change. *Science*
451 **353**, aad8466 (2016).
- 452 14. Maitner, B. *et al.* A global assessment of the Raunkiæran shortfall in plants: geographic
453 biases in our knowledge of plant traits. *New Phytologist* **240**, 1345–1354 (2023).

- 454 15. Thomas, H. J. *et al.* Global plant trait relationships extend to the climatic extremes of the
455 tundra biome. *Nature communications* **11**, 1351 (2020).
- 456 16. Právělie, R. Drylands extent and environmental issues. A global approach. *Earth-Science*
457 *Reviews* **161**, 259–278 (2016).
- 458 17. Maestre, F. T. *et al.* Biogeography of global drylands. *New Phytologist* **231**, 540–558
459 (2021).
- 460 18. Chai, R. *et al.* Human-caused long-term changes in global aridity. *npj Climate and*
461 *Atmospheric Science* **4**, 65 (2021).
- 462 19. Lian, X. *et al.* Multifaceted characteristics of dryland aridity changes in a warming world.
463 *Nature Reviews Earth & Environment* **2**, 232–250 (2021).
- 464 20. Reynolds, J. F. Desertification. in *Encyclopedia of Biodiversity* (ed. Levin, S. A.) 61–78
465 (Elsevier, New York, 2001).
- 466 21. Van Bodegom, P. M., Douma, J. C. & Verheijen, L. M. A fully traits-based approach to
467 modeling global vegetation distribution. *Proc. Natl. Acad. Sci. U.S.A.* **111**, 13733–13738
468 (2014).
- 469 22. Le Bagousse-Pinguet, Y. *et al.* Testing the environmental filtering concept in global
470 drylands. *Journal of Ecology* **105**, 1058–1069 (2017).
- 471 23. Noy-Meir, I. Desert Ecosystems: Environment and Producers. *Annu. Rev. Ecol. Syst.* **4**, 25–
472 51 (1973).
- 473 24. Marks, C. O. & Lechowicz, M. J. Alternative Designs and the Evolution of Functional
474 Diversity. *The American Naturalist* **167**, 55–66 (2006).
- 475 25. Volaire, F. A unified framework of plant adaptive strategies to drought: Crossing scales
476 and disciplines. *Global Change Biology* **24**, 2929–2938 (2018).
- 477 26. Gross, N. *et al.* Functional trait diversity maximizes ecosystem multifunctionality. *Nature*
478 *ecology & evolution* **1**, 0132 (2017).
- 479 27. Wright, I. J. *et al.* The worldwide leaf economics spectrum. *Nature* **428**, 821–827 (2004).
- 480 28. Fernández-Martínez, M. From atoms to ecosystems: elementome diversity meets
481 ecosystem functioning. *New Phytologist* **234**, 35–42 (2022).
- 482 29. Peñuelas, J. *et al.* The bioelements, the elementome, and the biogeochemical niche. *Ecology*
483 **100**, e02652 (2019).

- 484 30. Baxter, I. & Dilkes, B. P. Elemental Profiles Reflect Plant Adaptations to the Environment.
485 *Science* **336**, 1661–1663 (2012).
- 486 31. White, P. J. & Brown, P. Plant nutrition for sustainable development and global health.
487 *Annals of botany* **105**, 1073–1080 (2010).
- 488 32. Kaspari, M., De Beurs, K. M. & Welte, E. A. R. How and why plant ionomes vary across
489 North American grasslands and its implications for herbivore abundance. *Ecology* **102**,
490 e03459 (2021).
- 491 33. Lanning, M. *et al.* Intensified vegetation water use under acid deposition. *Sci. Adv.* **5**,
492 eaav5168 (2019).
- 493 34. Gollack, D., Li, C., Mohan, H. & Probst, N. Tolerance to drought and salt stress in plants:
494 unraveling the signaling networks. *Frontiers in plant science* **5**, 151 (2014).
- 495 35. Morales, F., Pavlovič, A., Abadía, A. & Abadía, J. Photosynthesis in Poor Nutrient Soils,
496 in Compacted Soils, and under Drought. in *The Leaf: A Platform for Performing*
497 *Photosynthesis* (eds. Adams Iii, W. W. & Terashima, I.) vol. 44 371–399 (Springer
498 International Publishing, Cham, 2018).
- 499 36. Mládková, P., Mládek, J., Hejduk, S., Hejcman, M. & Pakeman, R. J. Calcium plus
500 magnesium indicates digestibility: the significance of the second major axis of plant
501 chemical variation for ecological processes. *Ecology Letters* **21**, 885–895 (2018).
- 502 37. Boyd, R. Elemental defenses of plants by metals. *Nature Education Knowledge* **1**, (2010).
- 503 38. Blonder, B., Lamanna, C., Violle, C. & Enquist, B. J. The n -dimensional hypervolume.
504 *Global Ecology and Biogeography* **23**, 595–609 (2014).
- 505 39. Moles, A. T. *et al.* Correlations between physical and chemical defences in plants: tradeoffs,
506 syndromes, or just many different ways to skin a herbivorous cat? *New Phytologist* **198**,
507 252–263 (2013).
- 508 40. Briske, D. D. Strategies of plant survival in grazed systems: a functional interpretation. *The*
509 *ecology and management of grazing systems* 37–67 (1996).
- 510 41. Körner, C. *Alpine Plant Life*. (Springer Berlin Heidelberg, Berlin, Heidelberg, 2003).
511 doi:10.1007/978-3-642-18970-8.

- 512 42. Grime, J. P. Evidence for the Existence of Three Primary Strategies in Plants and Its
513 Relevance to Ecological and Evolutionary Theory. *The American Naturalist* **111**, 1169–
514 1194 (1977).
- 515 43. He, H., Bleby, T. M., Veneklaas, E. J., Lambers, H. & Kuo, J. Precipitation of calcium,
516 magnesium, strontium and barium in tissues of four Acacia species (Leguminosae:
517 Mimosoideae). *PLoS one* **7**, e41563 (2012).
- 518 44. Han, W. X., Fang, J. Y., Reich, P. B., Ian Woodward, F. & Wang, Z. H. Biogeography and
519 variability of eleven mineral elements in plant leaves across gradients of climate, soil and
520 plant functional type in China: Biogeography and variability of leaf chemistry. *Ecology*
521 *Letters* **14**, 788–796 (2011).
- 522 45. Michalet, R., Le Bagousse-Pinguet, Y., Maalouf, J. & Lortie, C. J. Two alternatives to the
523 stress-gradient hypothesis at the edge of life: the collapse of facilitation and the switch from
524 facilitation to competition. *J Vegetation Science* **25**, 609–613 (2014).
- 525 46. Rietkerk, M. & van de Koppel, J. Alternate stable states and threshold effects in semi-arid
526 grazing systems. *Oikos* 69–76 (1997).
- 527 47. Abades, S. R., Gaxiola, A. & Marquet, P. A. Fire, percolation thresholds and the savanna
528 forest transition: a neutral model approach. *Journal of Ecology* **102**, 1386–1393 (2014).
- 529 48. Berdugo, M. *et al.* Aridity preferences alter the relative importance of abiotic and biotic
530 drivers on plant species abundance in global drylands. *Journal of Ecology* **107**, 190–202
531 (2019).
- 532 49. Chesson, P. Mechanisms of Maintenance of Species Diversity. *Annu. Rev. Ecol. Syst.* **31**,
533 343–366 (2000).
- 534 50. Biggs, C. R. *et al.* Does functional redundancy affect ecological stability and resilience?
535 A review and meta-analysis. *Ecosphere* **11**, e03184 (2020).

536

537 **Figure Captions**

538 **Fig. 1: A survey of plant trait diversity across global dryland rangelands.** The database
539 included 1,347 observations of perennial plant species, which provided a complete set of
540 measurements for the 20 traits (see Supplementary Table 3 for details). The color of the dots
541 represented the aridity level of each of the 98 dryland sites where plant traits have been
542 measured. Each site included three to four plots locally distributed along a grazing gradient
543 (326 plots surveyed in total, see Methods). The size of the dots indicated the number of species
544 sampled in each plot. The selected sites were globally distributed across all latitudes and
545 continents (except Antarctica), and are representative of the wide variation in climates, soil
546 properties, and vegetation types found across global drylands^{6,17}. Aridity = 1 - Aridity index
547 (precipitation/potential evapotranspiration).

548

549 **Fig. 2: Global increase in dryland plant trait diversity driven by aridity and grazing.** Panel
550 a shows how aridity impacts on the size of the trait hypervolume, a measure of trait diversity
551 (see Methods). We found a significant, non-linear increase in the size of the hypervolume size
552 once an aridity threshold ~ 0.7 was crossed. Dashed and dotted lines represent the mean location
553 of the threshold and 95% Confidence Interval, respectively (see Supplementary Table 5 for
554 additional detailed results). Colored dots represent bootstrapped values for trait hypervolume
555 for each aridity level. Panel b compares the hypervolume size below and above this aridity
556 threshold. After crossing the ~ 0.7 aridity threshold, the hypervolume increased by 88.1 %
557 because it included not only most of the trait variability observed under low aridity conditions
558 (only 19.9 % of uniqueness), but also 57.3% of trait diversity that only occurs in the most arid
559 conditions. Panel c shows the bootstrapped values for trait hypervolume for each grazing
560 pressure level. Different letters indicate significant differences among grazing pressure levels.

561

562 **Fig. 3: Abrupt changes in trait covariations after crossing the ~ 0.7 aridity threshold.** Panel
563 a shows how the strength of trait covariations, measured using a phenotypic integration index
564 (see Methods), decreased with aridity. We found a significant, non-linear decline at aridity
565 values ~ 0.7 (see Supplementary Table 5 for more detailed results). Dashed and dotted lines
566 represent the mean location of the threshold and its 0.95 confidence interval, respectively.
567 Colored dots represent bootstrapped values for trait covariation for each aridity level. Panel b

568 shows the bootstrapped values for trait covariation for each grazing pressure level. Different
569 letters indicate significant differences among grazing pressure levels.

570

571 **Fig. 4: Interactions between grazing and aridity drive trait covariation and diversity**
572 **across global drylands.** Panels a and b show how grazing modulates the hypervolume size and
573 trait covariation in response to aridity. Panels c and d show the bootstrapped location of the
574 aridity-threshold at each grazing level with confidence intervals for hypervolume and trait
575 covariation, respectively. We used generalized least squares models to test for grazing effect in
576 panels (c, d). Different letters indicate significant ($P < 0.05$) differences among grazing pressure
577 levels. Grazing both changed the shape of the aridity response (see Supplementary Table 9 for
578 model selection for each grazing level) and the location of the threshold (colored dashed lines).
579 For instance, significant threshold-responses were observed under grazing (low, medium and
580 high grazing pressures) on trait hypervolume (panels a, c) while trait hypervolume remained
581 constantly low as aridity increased and increased linearly when grazing was removed (ungrazed
582 plots). For trait covariation (panels b, d), the thresholds appeared at lower aridity levels under
583 increasing grazing pressure.

584

585 **Methods**

586 Further details on methods are given in the Supplementary Information.

587

588 **Study site selection**

589 Our study focused on drylands, areas where rainfall is < 65% of the evaporative demand⁵¹. We
590 surveyed 98 dryland sites located in 25 countries from six continents (Algeria, Argentina,
591 Australia, Botswana, Brazil, Canada, Chile, China, Ecuador, Hungary, Iran, Israel, Kazakhstan,
592 Kenya, Mexico, Mongolia, Namibia, Niger, Palestine, Peru, Portugal, South Africa, Spain,
593 Tunisia, and the United States of America) (Figure 1). Site selection captured most of the aridity
594 conditions, vegetation (shrublands, grasslands, open woodlands, savannahs, and steppes) and
595 soil types that can be found in drylands worldwide (see refs.^{6,52} for more detailed explanation
596 on site selection). At each of the 98 study sites surveyed, three to four 45 m × 45 m plots (total
597 N = 326 plots) were selected along a local grazing gradient (ungrazed, low, medium, and high
598 grazing pressure), which was largely driven by livestock (but also included native herbivores⁶).
599 Each grazing gradient was established using the distance to artificial water points and grazing
600 enclosures when available (see ref.⁶ for a detailed assessment of the validation of the local
601 grazing gradients surveyed). In our dataset, aridity was defined as 1 - aridity index (AI, mean
602 annual precipitation/potential evapotranspiration⁵¹) following ref.⁵. Aridity ranged between
603 0.48 (wettest) to 0.99 (driest) across the surveyed drylands. This aridity range corresponds to a
604 gradient of mean annual precipitation between 891 and 29 mm/yr, and to a gradient of mean
605 annual temperature between -1.2 and 29.2°C. Our survey also captured most of the variation in
606 grazing pressure that can be found across dryland rangelands worldwide⁶.

607

608 **Plant trait sampling**

609 Fieldwork was conducted between January 2016 and September 2019. Vegetation surveys were
610 carried out after the main rainfall season at each site to ensure surveying during (or just after)
611 the main peak biomass. This approach allowed us to standardize the sampling while accounting
612 for differences in vegetation phenology among contrasted biogeographical regions, continents,
613 and hemispheres. We restricted our study to perennial plants because they represent 94% of the
614 plant species on earth⁵³ and are instrumental in maintaining the functioning of drylands^{26,54-56}.

615 We focused on 20 continuous traits related to the morphological and chemical diversity
616 of plants, which were measured following the most updated standardized protocols^{57,58}. These
617 traits included: i) whole-plant and leaf size related traits^{1,59} (maximum plant height [H, cm],
618 plant lateral spread [LS, cm²], leaf length [LL, cm] and leaf area [LA, cm²]); ii) leaf traits related
619 to carbon-economy and herbivory^{27,32,40,60,61} (Specific leaf area [SLA, cm².g⁻¹], leaf dry matter
620 content [LDMC, g.g⁻¹]); and iii) the foliar concentration of 14 chemical elements that
621 characterize the plant elementome^{28,29,32,62} (C, N, P, K, Mg, Ca, Zn, S, Na, Cu, Fe, Al, Mn, and
622 Ba). These traits were measured *in situ* within each of the 326 plots. To do so, four 45 m
623 transects oriented downslope were established within each plot, and spaced 10 m apart. We
624 then placed 25 contiguous quadrats (1.5 m × 1.5 m) along each transect (100 quadrats per plot).
625 Trait measurements were performed on five quadrats randomly selected in each transect (i.e.,
626 five quadrats x four transects = 20 quadrats per plot). In each quadrat, we selected the most
627 developed individual of each perennial species present. Our sampling protocol is highly suitable
628 to account for both local trait abundances (because frequent species will have more samples
629 than rare species^{63,64}) and between-plot intraspecific trait variability⁶⁵. See ref.⁵² for a detailed
630 description of the sampling protocol followed.

631 We measured plant height, i.e. the height of the selected individual from the ground to
632 the highest leaves belonging to the vegetative part of the plant; and the lateral spread using two
633 perpendicular measurements of plant width. On the same individual, we then sampled mature
634 and undamaged leaves at the top of the plant to ensure a development under full-light conditions
635 (sampled leaf surface was always > 2 cm²). Leaves were stored in moistened plastic bags and
636 brought to the laboratory for rehydration, before leaf area and leaf mass measurements.

637 We measured the leaf area of each sampled individual by taking pictures of the collected
638 leaves flattened below a glass sheet, and analyzed them using the freeware ImageJ⁶⁶
639 (<https://imagej.nih.gov/ij/index.html>; see ref.⁵² for additional details). Leaf fresh and dry mass
640 for each sampled individual were obtained by weighing before and after oven drying at 60 °C
641 for 48 h. Then, dry leaves were grouped by species within each plot in paper bags and were
642 shipped to the laboratory of Rey Juan Carlos University in Móstoles (Spain) for chemical
643 analyses. These shipments were carried out according to national and international regulations;
644 exporting permits were obtained for each country (when required) and importing permits to
645 Spain were obtained for every shipment by the Spanish Ministry of Agriculture, Fisheries and
646 Food.

647 Once in the laboratory, oven-dried leaves were ground in a homogenizer (Precellys®
648 24; Bertin Technologies, Montigny-le-Bretonneux, France) and analyzed for total nitrogen and
649 total carbon on a EuroEA3000 elemental analyser (EuroVector, Pavia, Italy). Total chemical
650 elements in leaves (P, K, Mg, Ca, Cu, Zn, S, Na, Fe, Al, Mn, and Ba) were analyzed by
651 inductively coupled plasma optical emission spectrometry with a Perkin Elmer Optima 4300
652 DV (Perkin Elmer, Waltham, Massachusetts, USA) after open-vessel nitric-perchloric acid wet
653 digestion. At the end of this procedure, we obtained the foliar concentration of the 14 elements
654 for each species sampled in each plot.

655

656 **Plant cover and soil properties measurements**

657 We quantified vegetation cover in each plot using the line-point intercept method⁵². We
658 recorded points located every 20 cm along each of the four transects for a total of 225 points
659 per transect (900 points per plot; see ref. 54 for additional details on this survey). Vegetation
660 cover was calculated as the proportion of points where perennial plants were recorded.

661 We also quantified the elemental concentrations of the soil beneath plant canopies in
662 each of the 326 plots surveyed in the peak of the dry season to ensure that the data obtained
663 across sites were as standardized and comparable as possible⁶. At each plot, five 50 cm × 50
664 cm quadrats were randomly placed under the canopy of the dominant (in terms of % cover)
665 perennial plant species. A composite topsoil sample consisting of five 145 cm³ soil cores (0-
666 7.5 cm depth) was collected from each quadrat, bulked, and homogenized in the field (five
667 composite samples per plot were obtained). After field collection, the soil samples were taken
668 to the laboratory, where they were sieved (2 mm mesh). Once sieved, samples were air-dried
669 for one month and stored for physico-chemical analyses. Dried soil samples from all the
670 countries were shipped to the laboratory of Rey Juan Carlos University in Móstoles (Spain) for
671 analyses. Once in the laboratory, replicated soil samples were bulked to obtain a composite
672 sample per plot. Total C and N concentration in soils was determined on ball-milled soils by
673 dry combustion, gas chromatography and thermal conductivity detection, after removing
674 carbonates by acid fumigation. Total P, K, Mg, Ca, Cu, Zn, S, Na, Fe, Al, Mn, and Ba were
675 extracted by open-vessel nitric-perchloric acid wet digestion, re-suspended in water, and
676 measured by inductively coupled plasma optical emission spectrometry^{67,68} (ICP-OES Perkin
677 Elmer Optima 4300 DV).

678 Soil pH was measured in all the soil samples with a pH meter, in a 1: 1 soil to water
679 (w:v) suspension⁵². Soil texture (sand, clay, and silt content) was measured according to ref.⁶⁹.
680 The three textural variables measured (sand, clay, and silt) were highly intercorrelated
681 (Spearman $\rho_{\text{sand-silt}} = -0.987$, $P < 0.001$; Spearman $\rho_{\text{sand-clay}} = -0.851$, $P < 0.001$; Spearman $\rho_{\text{silt-}$
682 $\text{clay}} = 0.766$, $P < 0.001$). Thus, we selected just one of these fractions (sand), to use in our data
683 analyses because this fraction is less prone to measurement errors given the method used.

684

685 **Data management and gap-filling procedure**

686 We compiled a database of 133,769 trait measurements, where each species in each plot was
687 tagged as a unique ID (Supplementary Table 3). Species taxonomy was standardized according
688 to World of Flora (WFO (2023): World Flora Online. <http://www.worldfloraonline.org>). 99.5%
689 of the individual plants were identified at the genus level, and 93.6% at the species level. We
690 used pseudo-species names for the 6.4% of species that could not be identified. To ensure a
691 high level of data quality, all trait measurements were inspected using a semi-automated
692 procedure and corrected when possible following guidelines from ref.¹¹. Specifically, we
693 looked for potential systematic errors, including wrong units or the presence of aberrant traits
694 values for each species and trait measured.

695 Morphological traits (H, LS, LL, LA, SLA, LDMC) were available at the individual
696 level (20,961 individual plants measured). Traits related to leaf nutrients were available at the
697 plot level for each species. To homogenize the level of analysis for all traits, we averaged
698 individual morphological measurements to obtain a single trait value for each species in each
699 of the 326 plots. For plant H and LS, we also recorded the maximum value observed in each
700 plot and for each species to characterize plant species maximum H and LS following ref.⁵⁷.

701 Data completeness varied among traits (Supplementary Table 3) but overall offered a
702 high degree of representativeness and geographical coverage at a global scale (Figure 1). We
703 did not have missing data for morphological traits (H, LS, LL). The levels of data completeness
704 for LA, SLA, LDMC were very high: 95%, 93%, and 89%, respectively. Missing data for these
705 variables were mainly due to methodological reasons, such as the inability to ensure a proper
706 leaf rehydration when measuring leaf fresh mass for LDMC. The amount of leaf dry material
707 sampled in the field was lower than the minimum required for some analyses for rare species
708 (for which the leaves of less than three individuals per plot were sampled). Thus, the number
709 of trait samples also differed among leaf nutrients (CN vs. other macro- and microelements)

710 due to the amount of leaf dry material available for analyses (2 mg of dry mass for C/N analyses
711 vs. 800 mg of dry mass for other elements). In total, the level of data completeness for chemical
712 traits was > 70% for C and N concentration in leaves and > 50 % for other macro and
713 microelements (Supplementary Table 3).

714 Data completeness is a fundamental prerequisite of trait covariation analyses because
715 multivariate analyses require a full set of trait information for all species considered. Indeed, a
716 missing value for one trait leads to systematic deletion of the whole species. Therefore, a gap-
717 filling procedure in the data trait matrices is a suitable approach to reduce this problem⁷⁰⁻⁷².
718 Here, we used a highly conservative gap-filling procedure based on the following criteria: i) we
719 used only trait data measured from our trait sampling, i.e. we did not retrieve trait data from
720 external databases such as TRY¹¹; ii) the gap-filling procedure was performed within species
721 in all cases (i.e., only when trait values were available for the same species in another plot); and
722 iii) we developed an algorithm to optimize the gap-filling procedure according to both aridity
723 and grazing levels instead of using phylogenetic relatedness⁷³. Specifically, when a trait value
724 is missing for a given species in a given plot, the algorithm allows filling the missing data by
725 maximizing the match between the species trait value and the local environmental conditions
726 (see all details of the gap-filling procedure in Supplementary Text 3; Supplementary Figures
727 13-15). Gap-filling significantly improved data representativeness by increasing the number of
728 species considered (Supplementary Table 3) without biasing the trait database. Indeed, we
729 observed remarkably low imputation errors (< 10%) for most chemical traits, indicating that
730 within species trait variability of the plant elementome is negligible compared to what is
731 observed across species (see additional results in Supplementary Text 3; Supplementary Figures
732 7-8).

733 At the end of the procedure, a total of 1,347 observations of dryland plant species
734 measured across the 326 plots with the complete set of traits were available for analyses
735 (compared to 887 observations before gap-filling, see Supplementary Table 3). The n = 1,347
736 observations were consistently used in all main analyses.

737

738 **Statistical analysis**

739 *Characterizing the dryland trait space*

740 To quantify the trait diversity of dryland plant species, we first determined the fundamental trait
741 dimensions along which dryland plant species segregate. To do this, we ran a series of principal

742 component analyses (PCAs) using the complete set of measured traits (Extended Data Figure
743 1) and plant chemical elements only (Supplementary Figure 5). Traits were log-transformed
744 and scaled before analysis¹² (see the distribution of each trait in Supplementary Figures 2-4).
745 We used the Horn's parallel analysis from the R package *paran*⁷⁴ to determine the
746 dimensionality of the PCAs¹², and applied a varimax rotation procedure to facilitate the
747 interpretation of the results.

748 PCAs are standard tools in trait spectrum analyses^{1,12,15,75}. They efficiently summarize
749 the covariations and trade-offs observed among multiple traits by representing the trait loadings
750 (arrows in Extended Data Figure 1) along the PCA axes (calculated from the eigenvectors of
751 each trait and the eigenvalues of each axis). The % of variance explained by each selected axis
752 represents the importance of each PCA dimension in explaining the observed trait variability
753 across species. Eigenvalues were further used to calculate an index of phenotypic integration,
754 which summarizes the strength of trait covariation⁷⁶⁻⁷⁸. This phenotypic integration index was
755 calculated using the variance of the eigenvalues as:

756

$$757 \quad Var(\gamma) = \sum_{i=1}^N (\gamma_i - 1)^2 / N \quad \text{equation 1}$$

758

759 where γ_i is the eigenvalue from the i-th dimension and N is the number of traits⁷⁹. We used the
760 eigenvalue of the un-rotated PCA to compute the phenotypic integration index. Higher values
761 of this index indicate stronger covariations among N traits. When traits are uncorrelated,
762 eigenvalues are similar and exhibit low variance. When traits are highly correlated, the first
763 eigenvalue is much higher than the other eigenvalues, leading to high variance. PCA axes also
764 provide information on the hypervolume^{1,38,80,81} occupied by the studied species in a n-
765 dimensional trait space, and thus the size of the hypervolume provides a measure of the trait
766 diversity observed for a given species pool⁸⁰. In this study, we used both hypervolumes and
767 trait covariations to quantify the effects of aridity and grazing on the spectrum of plant traits
768 observed in global drylands.

769

770 *Evaluating the impacts of aridity on the dryland plant trait space*

771 We used a sliding window analysis to evaluate how the hypervolume and trait covariation
772 changed along the aridity gradient evaluated. This analysis is well suited to investigate how the

773 correlation between different variables (here traits) change according to a third predictor (here
774 aridity), and to evaluate whether these changes are linear or abrupt^{48,82,83}. To do so, we first
775 ordered the 326 plots surveyed according to their aridity level. We then selected all plots located
776 within an aridity window of 0.1 (roughly equivalent to 19% of the total aridity gradient captured
777 in our survey), starting from the lowest aridity value observed in our dataset. The width of the
778 aridity window used was selected to ensure: i) enough statistical power (307 observations of
779 dryland plant species on average within each window; with min = 103 and max = 473); ii) that
780 the species pools selected in each window originated from plots characterized by different
781 grazing pressure levels; and iii) that the selected species belonged to contrasted biogeographical
782 regions across the world. Indeed, each aridity window included on average 19 sites (min = 8;
783 max = 32) originated from different regions of the world to avoid spatial autocorrelation, see
784 Figure 1). Therefore, our sliding windows analysis operates at a global scale to evaluate how
785 global increases in aridity and grazing pressure influence the trait pool in drylands worldwide.

786 For each aridity window, we calculated the strength of trait covariations using the same
787 PCA procedure as explained above and the diversity of trait values observed within this aridity
788 range. We randomly sampled $n = 100$ observations within the window and extracted the
789 eigenvalue of the significant selected axes, calculating their variance to obtain an index of
790 phenotypic integration. We repeated the random sampling of $n = 100$ observations for 100 times
791 within each window to calculate the confidence interval of the index for each aridity window.
792 We used the same procedure to calculate the hypervolume using the R package *Hypervolume*⁸¹.
793 To calculate the hypervolume, we used the PCA coordinates as trait values for the five
794 dimensions of the dryland plant spectrum described in Extended Data Figure 4. We then moved
795 the sliding window toward higher aridity levels of 0.01 by both adding the plots scoring the
796 next aridity value and removing the plots with the lowest aridity. We repeated this analysis as
797 many times as plots remained along the aridity gradient. We then plotted the results and tested
798 how trait covariations in the dryland species pool and their diversity changed along the aridity
799 gradient.

800 We evaluated whether the observed trait responses along the aridity gradient truly
801 corresponded to an aridity-threshold by fitting threshold models using the R package *chnngpt*⁸⁴.
802 In essence, these models find a breakpoint in the data by dividing it according to a predictor
803 value (here aridity) and using two different fitting functions at each side of the breakpoint. To
804 assess whether these threshold models were a better fit to the data than a linear model we used
805 the Bayesian information criterion (BIC), which measures the goodness of fit of the data based

806 on log-likelihood of the fitting functions considering the number of parameters used⁸². The
807 models exhibiting the lowest BIC values are the most parsimonious and provide the best fit.
808 Differences in BIC <2 represent similarly good models⁸⁵. Apart from a regular linear model,
809 we used a generalized additive model and five different threshold models for extracting the
810 BIC, each differing from each other by the functions fitted at both sides of the estimated
811 breakpoint: step (two intercept models, for which the differences in intercept were tested at the
812 breakpoint), segmented (two linear models in which the slope is changed at breakpoint),
813 segmented (two linear models in which both the slope and the intercept are changed at the
814 breakpoint), hinge model 12 (one linear model is fitted for the left part of the breakpoint and a
815 second degree polynomial is fitted for the right part), and hinge model 22 (two different second
816 degree polynomial models are fitted at both sides of the breakpoint). The model (either linear
817 or threshold-like) exhibiting the lowest BIC was considered the best model. Each of the
818 threshold models considered allows the identification of a breakpoint with associated 0.95
819 confidence interval (CI) as a parameter resulting from the model fitting. We considered the
820 aridity value at which a breakpoint was observed as the aridity threshold.

821 We observed non-linear, abrupt responses of trait covariations and hypervolumes at
822 aridity ~0.7 based on the breakpoint analyses described above (Figs. 2 and 3). To further
823 examine how aridity reshaped the dryland plant trait spectrum, we divided our data into two
824 subsets: below and above aridity = $0.7 \pm$ Confidence Interval (CI). We re-ran all the PCA
825 analyses explained above to evaluate how aridity changed the dimensionality of the trait
826 spectrum for these subsets of the data. We also re-calculated the hypervolume observed at low
827 and high aridity values, and quantified their overlap using the function
828 *hypervolume_overlap_statistics* in the R package *Hypervolume*⁸¹. This function provides the %
829 of overlap between distinct hypervolumes, as well as the % of uniqueness of each hypervolume.

830

831 *Assessing the impacts of grazing on the dryland plant trait space*

832 To test for the effects of grazing pressure, we calculated the index of trait covariation and the
833 hypervolumes for each grazing pressure level (ungrazed, low, medium, and high grazing
834 pressure). We used a bootstrap procedure and repeated the calculation 100 times to obtain the
835 confidence interval. We then tested whether different grazing levels showed contrasted values
836 of these indices using a generalized least squares model to account for heteroscedasticity (using
837 the function *gls* from the R package *nlme*⁸⁶). To represent how different grazing pressures may

838 alter the dryland plant trait space, we also re-ran the PCA analyses for each grazing pressure
839 level evaluated (from ungrazed to high grazing pressure). Finally, we tested whether grazing
840 pressure changed the shape and the location of the aridity threshold. To do so, we re-ran the
841 sliding windows analysis conducted above, but at each grazing level separately. We tested
842 whether grazing pressure (ungrazed, low, medium, and high grazing pressure) changed the
843 location of the threshold. We extracted the bootstrap distribution of the threshold at each
844 grazing pressure level, and tested, using generalized least square models, whether the location
845 of the threshold was significantly shifted along the aridity gradient compared to the overall
846 threshold found at aridity ~ 0.7 .

847

848 *Assessing the impacts of aridity and grazing on the soil elementome*

849 We examined how chemical elements in soils (the soil elementome) responded to changes in
850 aridity. We first conducted a PCA as explained above to evaluate how the concentrations of the
851 14 chemical elements in soils covary across the 326 sampled plots. We then extracted the PC
852 coordinate of each selected axis and evaluated how the soil elementome responded to grazing
853 and aridity using linear mixed effect models and the R package *lme4*⁸⁷. We considered in the
854 model the effect of grazing and aridity and used site as a random factor (random effect: 1|site),
855 allowing model intercept to vary among sites since plots belonging to the same site correspond
856 to a local grazing gradient that has been repeated across the 98 sites surveyed. Finally, we used
857 the same sliding windows procedure as explained above to test how soil chemical diversity
858 responded to aridity. All soil elements covaried along a unique PC axis accounting for 65.8%
859 of the total variation (Extended Data Figure 5a, b). Because computing hypervolumes in one
860 dimension is irrelevant⁸¹, we therefore computed the sliding window analysis only to test
861 whether covariation among multiple soil elements changed with increasing aridity (Extended
862 Data Figure 5c).

863

864 *Plant cover as a modulator of the effects of aridity and grazing on the dryland plant trait space*

865 We evaluated how changes in plant cover observed across global drylands once the ~ 0.7 aridity
866 threshold is crossed impacted on plant trait diversity. We first tested how aridity and grazing
867 impacted plant cover using linear mixed effect models and the R package *lme4*⁸⁷. Our model
868 included aridity, grazing, and an interaction between them. Site was used as a random factor
869 (random effect: 1|site). The model also included a series of covariates known to impact plant

870 cover⁶ in drylands, such as latitude and longitude of our study sites, as well as their elevation
871 and topography (slope and aspect). We used the sine and cosine of the longitude and aspect to
872 avoid any bias due to intrinsic circularity of these predictors in the statistical models²² (i.e.,
873 Longitude (sin) and Longitude (cos) hereafter, respectively). We also considered two soil
874 master variables, i.e. sand content and soil pH^{22,88}. A quadratic term was considered for pH. All
875 predictors were scaled before analysis to facilitate the comparison of estimates.

876 The full model used was: lmer (Plant Cover ~ (1|site) + latitude + longitude (sin) +
877 longitude (cos) + exposure (sin) + exposure (cos) + slope + elevation + aridity*grazing + sand
878 + pH + pH²). Using this full model, we ran a model averaging procedure to select the set of
879 predictors that best explained variations in plant cover. To do this, we applied a multi-model
880 inference procedure using the *MuMIn* R package⁸⁹. This method allowed us to create a set of
881 models with all possible combinations of the initial variables, which were fitted using a
882 Maximum Likelihood procedure⁹⁰ and sorted according to the Akaike Information Criterion
883 (AIC). Aridity and grazing were the main drivers of plant cover in our analyses (Extended Data
884 Figure 6). Finally, we substituted aridity by plant cover in our sliding windows procedure to
885 test how plant cover influenced hypervolume and trait covariation (Extended Data Figure 7).

886

887 **Data and code availability**

888 Processed datasets generated during the current study, as well as the R code used to analyze
889 them, are available in the nextcloud.inrae repository:

890

891 <https://nextcloud.inrae.fr/s/qC4mjPPerQewADwD>

892 **References (Methods)**

- 893 51. ILRI, I. UNEP and ILC. 2021. *Rangelands Atlas. Nairobi Kenya: ILRI For more*
894 *information on the Atlas please contact: Fiona Flintan, Senior Scientist, ILRI f. flintan@*
895 *cgiar. org BY CC 4 (2021).*
- 896 52. Maestre, F. T. *et al.* The BIODESERT survey: Assessing the impacts of grazing on the
897 structure and functioning of global drylands. *Web Ecology* **22**, 75–96 (2022).
- 898 53. Poppenwimer, T., Mayrose, I. & DeMalach, N. Revising the global biogeography of annual
899 and perennial plants. *Nature* **624**, 109–114 (2023).
- 900 54. García-Palacios, P., Gross, N., Gaitán, J. & Maestre, F. T. Climate mediates the
901 biodiversity–ecosystem stability relationship globally. *Proc. Natl. Acad. Sci. U.S.A.* **115**,
902 8400–8405 (2018).
- 903 55. Maestre, F. T. *et al.* Plant Species Richness and Ecosystem Multifunctionality in Global
904 Drylands. *Science* **335**, 214–218 (2012).
- 905 56. Le Bagousse-Pinguet, Y. *et al.* Phylogenetic, functional, and taxonomic richness have both
906 positive and negative effects on ecosystem multifunctionality. *Proc. Natl. Acad. Sci. U.S.A.*
907 **116**, 8419–8424 (2019).
- 908 57. Cornelissen, J. H. C. *et al.* A handbook of protocols for standardised and easy measurement
909 of plant functional traits worldwide. *Aust. J. Bot.* **51**, 335–380 (2003).
- 910 58. Pérez-Harguindeguy, N. *et al.* Corrigendum to: New handbook for standardised
911 measurement of plant functional traits worldwide. *Aust. J. Bot.* **64**, 715–716 (2016).
- 912 59. Wright, I. J. *et al.* Global climatic drivers of leaf size. *Science* **357**, 917–921 (2017).
- 913 60. Deraison, H., Badenhausser, I., Börger, L. & Gross, N. Herbivore effect traits and their
914 impact on plant community biomass: an experimental test using grasshoppers. *Functional*
915 *Ecology* **29**, 650–661 (2015).
- 916 61. Cruz, P. *et al.* Leaf Traits as Functional Descriptors of the Intensity of Continuous Grazing
917 in Native Grasslands in the South of Brazil. *Rangeland Ecology & Management* **63**, 350–
918 358 (2010).
- 919 62. Salt, D. E., Baxter, I. & Lahner, B. Ionomics and the Study of the Plant Ionome. *Annu. Rev.*
920 *Plant Biol.* **59**, 709–733 (2008).

- 921 63. Gaucherand, S. & Lavorel, S. New method for rapid assessment of the functional
922 composition of herbaceous plant communities. *Austral Ecology* **32**, 927–936 (2007).
- 923 64. Gross, N., Börger, L., Duncan, R. P. & Hulme, P. E. Functional differences between alien
924 and native species: do biotic interactions determine the functional structure of highly
925 invaded grasslands? *Functional Ecology* **27**, 1262–1272 (2013).
- 926 65. Siefert, A. *et al.* A global meta-analysis of the relative extent of intraspecific trait variation
927 in plant communities. *Ecology Letters* **18**, 1406–1419 (2015).
- 928 66. Schneider, C. A., Rasband, W. S. & Eliceiri, K. W. NIH Image to ImageJ: 25 years of image
929 analysis. *Nat Methods* **9**, 671–675 (2012).
- 930 67. Varley, J. A. A Textbook of Soil Chemical Analysis By P. R. Hesse London: John Murray
931 (1971), pp. 520, £7·50. *Experimental Agriculture* **8**, 184–184 (1972).
- 932 68. Kuo, S. Phosphorus. in *Methods of Soil Analysis* 869–919 (John Wiley & Sons, Ltd, 1996).
933 doi:10.2136/sssabookser5.3.c32.
- 934 69. Kettler, T. a., Doran, J. w. & Gilbert, T. I. Simplified Method for Soil Particle-Size
935 Determination to Accompany Soil-Quality Analyses. *Soil Science Society of America*
936 *Journal* **65**, 849–852 (2001).
- 937 70. Penone, C. *et al.* Imputation of missing data in life-history trait datasets: which approach
938 performs the best? *Methods Ecol Evol* **5**, 961–970 (2014).
- 939 71. Poyatos, R., Sus, O., Badiella, L., Mencuccini, M. & Martínez-Vilalta, J. Gap-filling a
940 spatially explicit plant trait database: comparing imputation methods and different levels of
941 environmental information. *Biogeosciences* **15**, 2601–2617 (2018).
- 942 72. Jetz, W. *et al.* Monitoring plant functional diversity from space. *Nature Plants* **2**, 1–5
943 (2016).
- 944 73. Swenson, N. G. Phylogenetic imputation of plant functional trait databases. *Ecography* **37**,
945 105–110 (2014).
- 946 74. Dinno, A. PARAN: Stata module to compute Horn’s test of principal components/factors.
947 (2009).
- 948 75. Bueno, C. G. *et al.* Reply to: The importance of trait selection in ecology. *Nature* **618**, E31–
949 E34 (2023).

- 950 76. Laughlin, D. C. *et al.* Intraspecific trait variation can weaken interspecific trait correlations
951 when assessing the whole-plant economic spectrum. *Ecology and Evolution* **7**, 8936–8949
952 (2017).
- 953 77. Brown, A., Butler, D. W., Radford-Smith, J. & Dwyer, J. M. Changes in trait covariance
954 along an orographic moisture gradient reveal the relative importance of light- and moisture-
955 driven trade-offs in subtropical rainforest communities. *New Phytologist* **236**, 839–851
956 (2022).
- 957 78. Delhaye, G. *et al.* Interspecific trait integration increases with environmental harshness: A
958 case study along a metal toxicity gradient. *Functional Ecology* **34**, 1428–1437 (2020).
- 959 79. Cheverud, J. M., Wagner, G. P. & Dow, M. M. Methods for the Comparative Analysis of
960 Variation Patterns. *Systematic Biology* **38**, 201–213 (1989).
- 961 80. Blonder, B. Hypervolume concepts in niche- and trait-based ecology. *Ecography* **41**, 1441–
962 1455 (2018).
- 963 81. Blonder, B. *et al.* New approaches for delineating n -dimensional hypervolumes. *Methods*
964 *Ecol Evol* **9**, 305–319 (2018).
- 965 82. Berdugo, M., Gaitán, J. J., Delgado-Baquerizo, M., Crowther, T. W. & Dakos, V.
966 Prevalence and drivers of abrupt vegetation shifts in global drylands. *Proc. Natl. Acad. Sci.*
967 *U.S.A.* **119**, e2123393119 (2022).
- 968 83. Berdugo, M., Kéfi, S., Soliveres, S. & Maestre, F. T. Plant spatial patterns identify
969 alternative ecosystem multifunctionality states in global drylands. *Nature ecology &*
970 *evolution* **1**, 0003 (2017).
- 971 84. Fong, Y., Huang, Y., Gilbert, P. B. & Permar, S. R. chngpt: threshold regression model
972 estimation and inference. *BMC Bioinformatics* **18**, 454 (2017).
- 973 85. Schwarz, G. Estimating the Dimension of a Model. *The Annals of Statistics* **6**, 461–464
974 (1978).
- 975 86. Pinheiro, J. *et al.* Package ‘nlme’. *Linear and nonlinear mixed effects models, version*
976 **3**, 274 (2017).
- 977 87. Bates, D. *et al.* lme4: Linear Mixed-Effects Models using ‘Eigen’ and S4. (2024).
- 978 88. Maire, V. *et al.* Global effects of soil and climate on leaf photosynthetic traits and rates.
979 *Global Ecology and Biogeography* **24**, 706–717 (2015).

- 980 89. K. Barton, MuMIn: Model Selection and Model Averaging Based on Information
981 Criteria (AICc and alike) (R Package Version, 1–1, 2014).
- 982 90. Zuur, A. F., Ieno, E. N., Walker, N., Saveliev, A. A. & Smith, G. M. *Mixed Effects Models*
983 *and Extensions in Ecology with R*. (Springer, 2009).
- 984

985 **Acknowledgements**

986 This research was funded by the European Research Council (ERC Grant agreement 647038
987 1004 [BIODESERT]) and Generalitat Valenciana (CIDEGENT/2018/041). We acknowledge
988 Sainbileg Undrakhbold, Munkhbat Uuganbayar, Batbold Byambatsogt, Sanchir Khaliun,
989 Shijirbaatar Solongo, Bud Batchuluun, Michael Sloan, Sedona Spann, John Spence, Erika
990 Geiger, Isys Souza, Richard Onoo, Thiago Araújo, Mancha Mabaso, Percy Mutseka Lunga,
991 Louis Eloff, Julius Sebei, Dr Jorrie J. Jordaan, Dr Edwin Mudongo, Dr Vincent Mokoka,
992 Baltimore Mokhou, Thabang Maphanga, Dr Dave Thompson (SAEON), Dr Anke S. K. Frank,
993 Rose Matjea, Florian Hoffmann, Chris Goebel, Bruce Semple, Bobby Tamayo, Rebecca Peters,
994 Adriana Lozada Piña, Roxana Ledezma, Eduardo Vidal, Franco Perona, Julio M. Alcántara,
995 Armin Howell, Robin Reibold, Nick Melone, Megan Starbuck, Erika Geiger, Bush Heritage
996 Australia, the University of Limpopo, Comunidad Agrícola Quebrada de Talca, Conaf Chile,
997 South African Environmental Observation Network (SAEON) for assistance with field work
998 and plant identification, the South African Military for assistance with field work and/or
999 granting access to their properties, and the Scientific Services Kruger National Park. N.G. was
1000 supported by CAP 20-25 (16-IDEX-0001) and the AgreeSkills+ fellowship programme which
1001 1020 has received funding from the EU's Seventh Framework Programme under grant
1002 agreement N° FP7-609398 (AgreeSkills+ contract). F.T.M. acknowledges support from the
1003 King Abdullah University of Science and Technology (KAUST), the KAUST Climate and
1004 Livability Initiative, the University of Alicante (UADIF22-74 and VIGROB22-350), the
1005 Spanish Ministry of Science and Innovation (PID2020-116578RB-I00), and the Synthesis
1006 Center (sDiv) of the German Centre for Integrative Biodiversity Research Halle–Jena–Leipzig
1007 (iDiv). Y.L.B.-P. was supported by a Marie Skłodowska-Curie Actions Individual Fellowship
1008 (MSCA-1018 IF) within the European Program Horizon 2020 (DRYFUN Project 656035). H.S.
1009 is supported by a María Zambrano fellowship funded by the Ministry of Universities and
1010 European Union-Next Generation plan. L.W. acknowledges support from the US National
1011 Science Foundation (EAR 1554894). G.M.W. acknowledges support from the Australian
1012 Research Council (DP210102593) and TERN. M.B is supported by a Ramón y Cajal grant from
1013 Spanish Ministry of Science (RYC2021-031797-I). LvdB and KT were supported by the
1014 German Research Foundation (DFG) Priority Program SPP-1803 (TI388/14-1). A.F.
1015 acknowledges the financial support from ANID PIA/BASAL FB210006 and Millenium
1016 Science Initiative Program NCN2021-050. A.J. was supported by the Bavarian Research
1017 Alliance for travel and field work (BayIntAn UBT 2017 61). A.L. and L.K. acknowledge

1018 support from the German Research Foundation, DFG (grant CRC TRR228) and German
1019 Federal Government for Science and Education, BMBF (grants 01LL1802C and 01LC1821A).
1020 BB and SU were supported by the Taylor Family-Asia Foundation Endowed Chair in Ecology
1021 and Conservation Biology. PJR and AJM acknowledge support from Fondo Europeo de
1022 Desarrollo Regional through the FEDER Andalucía operative programme, FEDER-UJA
1023 1261180 project. E.M.-J. and C.P. acknowledge support from the Spanish Ministry of Science
1024 and Innovation (PID2020-116578RB-I00). D.J.E was supported by the Hermon Slade
1025 Foundation. J.D. and A.Rodríguez acknowledge support from the FCT (2020.03670.CEECIND
1026 and SFRH/BDP/108913/2015, respectively), as well as from the MCTES, FSE, UE, and the
1027 CFE (UIDB/04004/2021) research unit financed by FCT/MCTES through national funds
1028 (PIDDAC). S.R. acknowledges support from the U.S. Department of Energy (DE-SC-
1029 0008168), U.S. Department of Defense (RC18-1322), and the U.S. Geological Survey
1030 Ecosystems Mission Area. Any use of trade, firm, or product names is for descriptive purposes
1031 only and does not imply endorsement by the U.S. government. EHS acknowledges support from
1032 Mexican National Science and Technology Council (CONACYT PN 5036 and 319059). A.N.
1033 and C.B. acknowledge the support from FCT - Fundação para a Ciência e a Tecnologia
1034 (CEECIND/02453/2018/CP1534/CT0001, PTDC/ASP-SIL/7743/ 2020, UIDB/00329/2020),
1035 from AdaptForGrazing project (PRR-C05-i03-I-000035) and from LTsER Montado platform
1036 (LTER_EU_PT_001). Field work of GP and JMZ was supported by UNRN (PI 40-C-873).

1037 **Author contributions**

1038 N.G., F.T.M., and Y.L.B.-P. conceived this study. F.T.M., N.G., and Y.L.B.-P. designed and
1039 coordinated the global field survey. N.G., P.L., and Y.L.B.-P. developed the original idea of the
1040 analyses presented in the manuscript, with inputs from F.T.M., M.B., R.M., M.D-B., V.M.,
1041 E.M-J., H.S., S.S., and E.V.. F.J. developed the theoretical model on plant cover. Fieldwork
1042 was done by all co-authors with the assistance of M.G.G. for field site assessments. Laboratory
1043 analyses were done by V.O., B.G., S.A., C.P., M.G.G., and I.S.P. The trait database was built
1044 by N.G., R.M., and Y.L.B.-P. Data and code handling, curation, and verification were done by
1045 N.G, R.M. V.O., B.G., I.S.P., and Y.L.B.-P. Statistical analyses were performed by N.G., M.B.,
1046 and R.M. N.G., Y.L.B.-P., and F.T.M. wrote the first manuscript draft and all authors worked
1047 on the final version.

1048

1049 **Additional Information**

1050 Supplementary Information is available for this paper. Correspondence and requests for
1051 materials should be addressed to Nicolas Gross (nicolas.gross@inrae.fr), Fernando T. Maestre
1052 Gil (ft.maestre@gmail.com), Yoann Pinguet (yoann.pinguet@imbe.fr).

1053

1054 **Extended Data Captions**

1055 **Extended Data Figure 1. The trait space of global dryland rangelands.** The panels represent
1056 the probabilistic species distributions in the space defined by a Principal Component Analysis
1057 (PCA) on whole-plant and leaf size, and on leaf chemical traits. We show the dimensions related
1058 to plant size and leaf C-economy (a), and the additional, but independent dimensions related to
1059 the plant elementome (b and c) characterized by the concentration of 14 elements in plant
1060 leaves: C, N, P, Mg, Mn, Ca, Cu, Al, Ba, Fe, K, Na, S, and Zn. The dryland trait space displayed
1061 five major dimensions (Principal Components PC1 to PC5), accounting for 66.7 % of the total
1062 trait variation. Leaf traits related to leaf C-economy (PC1) and plant size (PC3) varied along
1063 two orthogonal dimensions and accounted for a total of 28.2% of trait variation (panel a). The
1064 plant elementome accounted for 55.5% of trait variation (panels b, c). While a dimension of the
1065 plant elementome covaried with the leaf C-economy dimension²⁷ (N-P-K on PC1), it also added
1066 three other orthogonal dimensions that were associated with important macro- and
1067 micronutrients (PC2, PC4, PC5). These findings show that a large fraction of trait diversity
1068 found across global drylands is not captured by plant size and leaf C-economy alone, but by the
1069 plant elementome (see Supplementary Figure 5 for an additional description of the elementome;
1070 Supplementary Figure 8 for the PCA ran without the gap-filling of the data; Supplementary
1071 Figure 7 for pictures of dryland plant species). The color gradient depicts the different species
1072 densities in the trait space (high and low density in red and fading yellow, respectively). The
1073 arrow length is proportional to the trait loadings. Each point represents the location of a species
1074 within the five-dimensional trait space for all the species surveyed (n = 1347). Abbreviations:
1075 maximum plant height, H; Lateral spread, LS; Leaf length, LL; leaf area, LA; specific leaf area,
1076 SLA; leaf dry matter content, LDMC. See also Supplementary Table 4 for detailed results.

1077

1078 **Extended Data Figure 2. Aridity reshuffles the trait space of global dryland rangelands.**
1079 We show how trait covariation changes along the aridity gradient using principal component
1080 analysis conducted for sites with aridity values located below (panels a and b) and above (panels
1081 c-e) the aridity threshold of ~0.7. The arrow length is proportional to the loadings of the traits
1082 considered. Four principal components were significantly selected at aridity values <0.7 (panels
1083 a and b) while five components were selected at aridity values >0.7 (panels c-e). See Extended
1084 Data Figure 1 for trait abbreviations and Supplementary Table 4 for detailed results.

1085

1086 **Extended Data Figure 3. Presence of grazers modulates the trait space of global dryland**
1087 **rangelands.** We show how trait covariation changes with increasing grazing pressure using
1088 Principal Component analysis. The arrow length is proportional to the loadings of the traits
1089 considered. Four and five principal components were significantly selected in ungrazed (panels
1090 j and k) and grazed (panels a-i) plots, respectively. See Extended Data Figure 1 for trait
1091 abbreviations and Supplementary Table 6 for detailed results. Low = low grazing pressure, Med
1092 = medium grazing pressure, and High = high grazing pressure.

1093

1094 **Extended Data Figure 4. Representation of the trait hypervolume before and after**
1095 **crossing the ~0.7 aridity threshold.** We show the 2D projection of the hypervolume for each
1096 pair of PCA dimensions shown in Extended Data Figure 1 (n-dimensions = 5, from PC1 to
1097 PC5). Colored dots represent the locations of each measured species within the trait space. The
1098 blue and the red large bright dots represented the centroids of each hypervolume before and
1099 after an aridity value of 0.7. Colored lines show the 0.95 confidence intervals of the
1100 hypervolume before and after this aridity value.

1101

1102 **Extended Data Figure 5. Response of elemental concentration in soils (the soil**
1103 **elementome) to aridity.** Soil elements covary across the 326 sampled plots along a unique
1104 Principal Component axis (PC1) that account for 65.8 % of soil total variation (see Methods).
1105 Panel a shows responses of the soil elementome, illustrated using the soil PC 1, to aridity. PC1
1106 shows a quadratic response to aridity with non-linear decrease occurring only in the most arid
1107 areas, i.e., those with aridity values > 0.8. Grazing did not modify this response. Panel b shows
1108 the PC coordinates of each element along PC1. Panel c shows how the soil elementome
1109 responded to aridity using a sliding windows analysis (see methods). We first ordered the 326
1110 plots according to their aridity level. We then defined an aridity window that represented 10%
1111 of the global aridity gradient and selected all plots within this aridity range (n > 30 plots in each
1112 window). We finally examined how the covariation of soil elements across plots changed as
1113 aridity increased. We found that aridity further increased the covariation of soil elements in the
1114 most arid rangelands surveyed. See Supplementary Table 7 for detailed results of model
1115 selections evaluating the response of the soil elementome to aridity.

1116

1117 **Extended Data Figure 6. Global decrease in plant cover driven by aridity and grazing.**
1118 Panel a shows the averaged model parameters (\pm se) for different predictors (i.e. aridity,
1119 grazing, soil, and geographical variables) on plant cover. Significant predictors do not cross the
1120 dotted line. Aridity and grazing were the main drivers of plant cover. Panels b and c illustrate
1121 the effects of aridity and grazing on plant cover. Dashed and dotted lines represent the mean
1122 location of the threshold and its 0.95 confidence interval, respectively. Plant cover decreased
1123 non-linearly at aridity \sim 0.7 and was the lowest under high grazing pressure.

1124

1125 **Extended Data Figure 7. Plant cover mediates the effect of aridity and grazing pressure**
1126 **on trait diversity across global dryland rangelands.** Panels show the response of trait
1127 diversity (hypervolume and trait covariation) to plant cover using a sliding window procedure
1128 (see Methods). Increasing plant cover decreased hypervolume and increased trait covariations,
1129 with a significant threshold value occurring at a plant cover value close to $50\% \pm$ CI (dashed
1130 lines, the dotted lines show its 0.95 percentile Confidence Interval, CI). See Supplementary
1131 Table 8 for detailed results of model selection evaluating the response of the plant elementome
1132 to plant cover.

1133

1134 **Main Figures**

1135

1136 **Figure 1.** A survey of plant trait diversity across global dryland rangelands.

1137

1138 **Figure 2.** Global increase in dryland plant trait diversity driven by aridity and grazing.

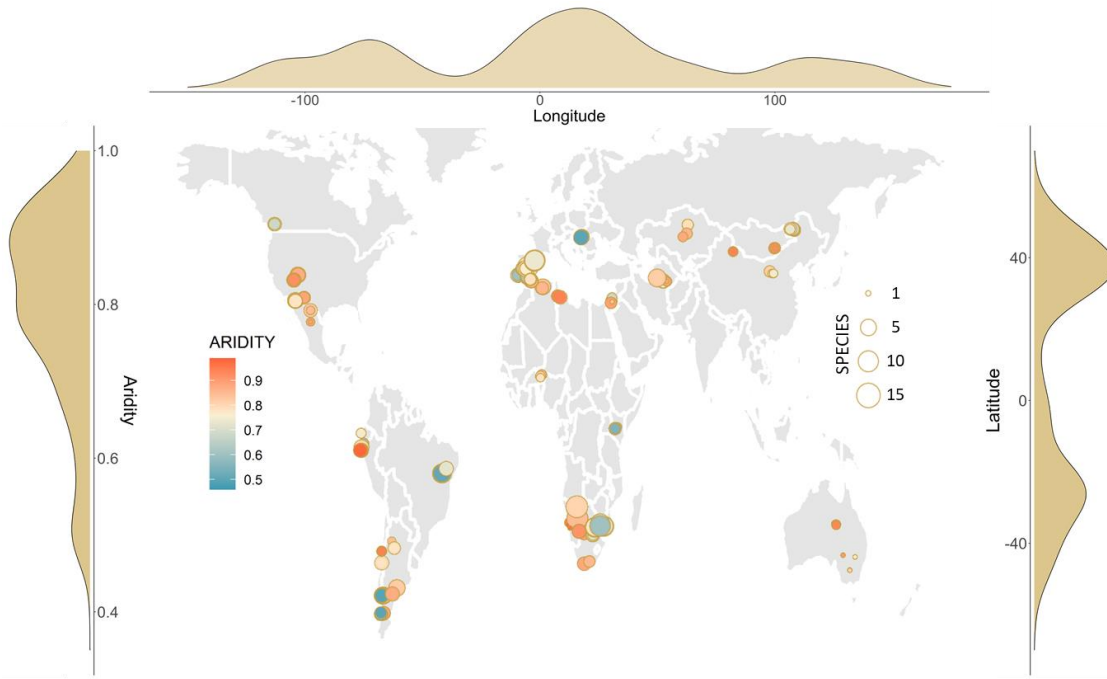
1139

1140 **Figure 3.** Abrupt changes in trait covariations after crossing the ~0.7 aridity threshold.

1141

1142 **Figure 4.** Interactions between grazing and aridity drive trait covariation and diversity across
1143 global drylands.

1144



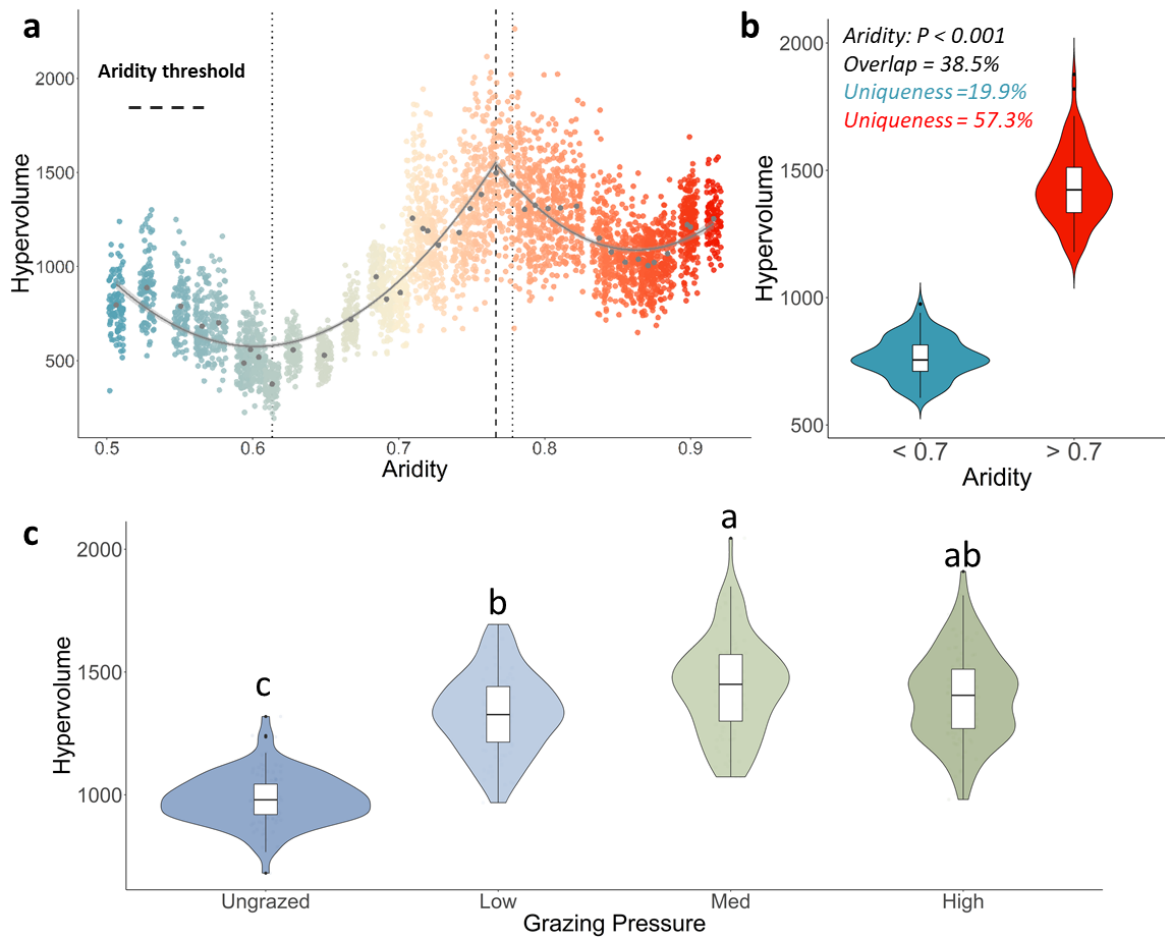
1145

1146

1147 **Figure. 1**

1148

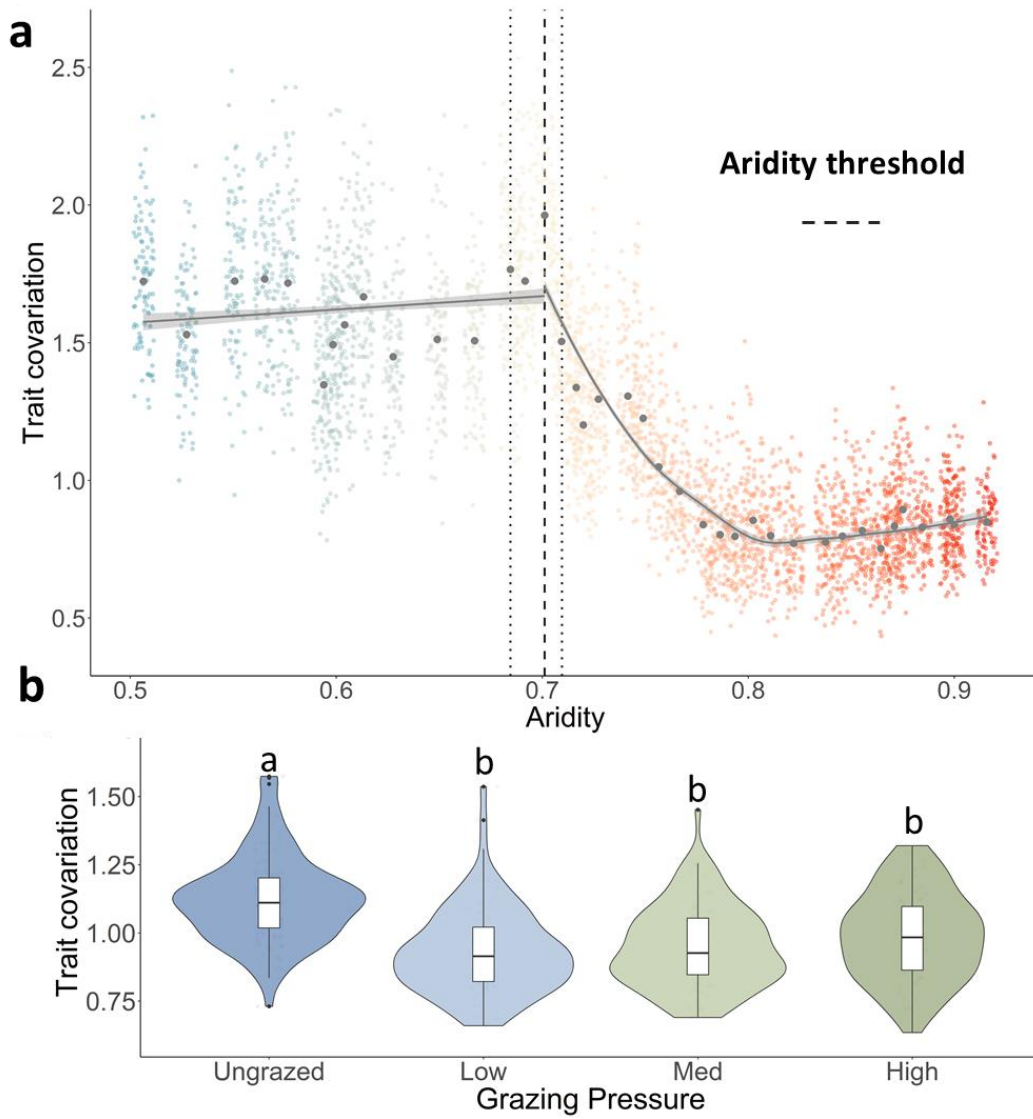
1149



1150

1151 **Figure. 2**

1152

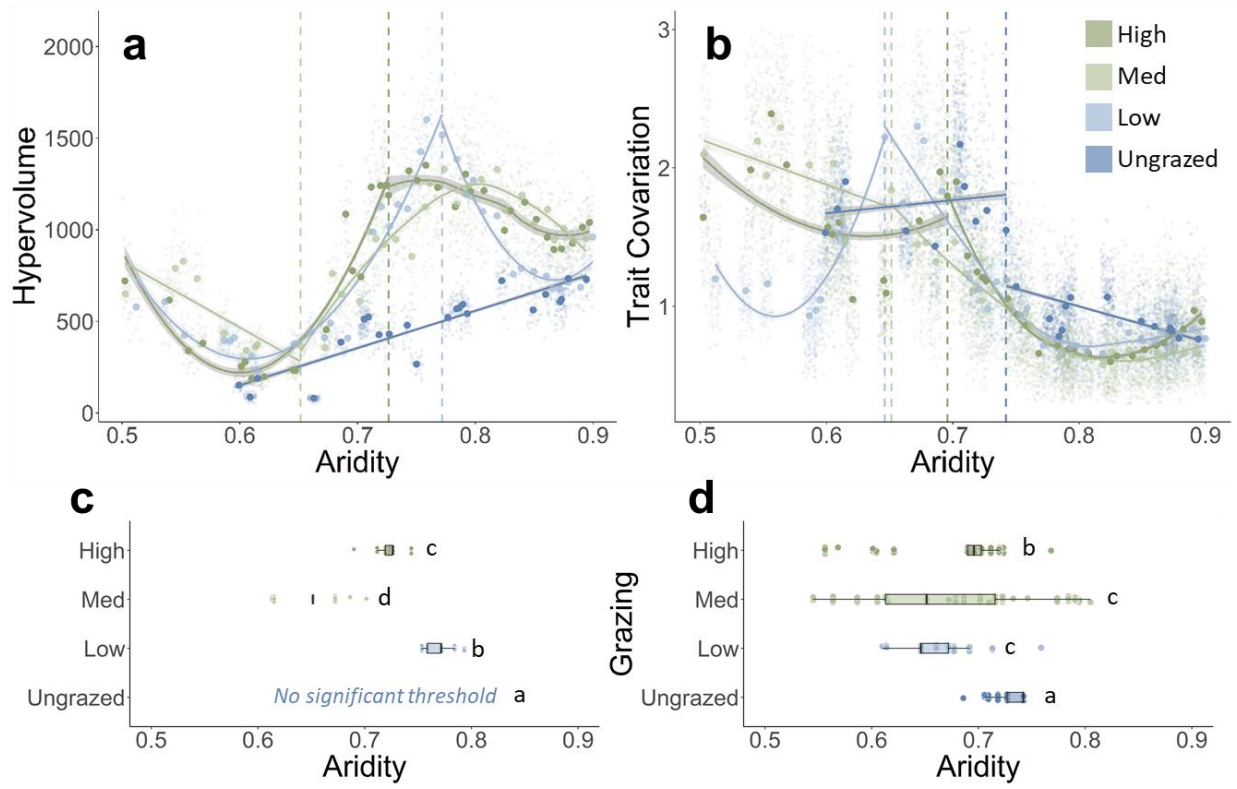


1153

1154 **Figure. 3**

1155

1156



1157

1158

1159 **Figure. 4**

1160

1161 **Extended Data Figures**

1162

1163 **Extended Data Figure 1.** The trait space of global dryland rangelands.

1164

1165 **Extended Data Figure 2.** Aridity reshuffles the trait space of global dryland rangelands.

1166

1167 **Extended Data Figure 3.** The presence of grazers modulates the trait space of global dryland
1168 rangelands.

1169

1170 **Extended Data Figure 4.** Representation of the trait hypervolume before and after crossing the
1171 ~0.7 aridity threshold

1172

1173 **Extended Data Figure 5.** Response of elemental concentration in soils (soil elementome) to
1174 aridity

1175

1176 **Extended Data Figure 6.** Global decreases in plant cover driven by aridity and grazing.

1177

1178 **Extended Data Figure 7.** Plant cover mediates the effect of aridity and grazing pressure on
1179 trait diversity across global drylands.

1180

1181

1182

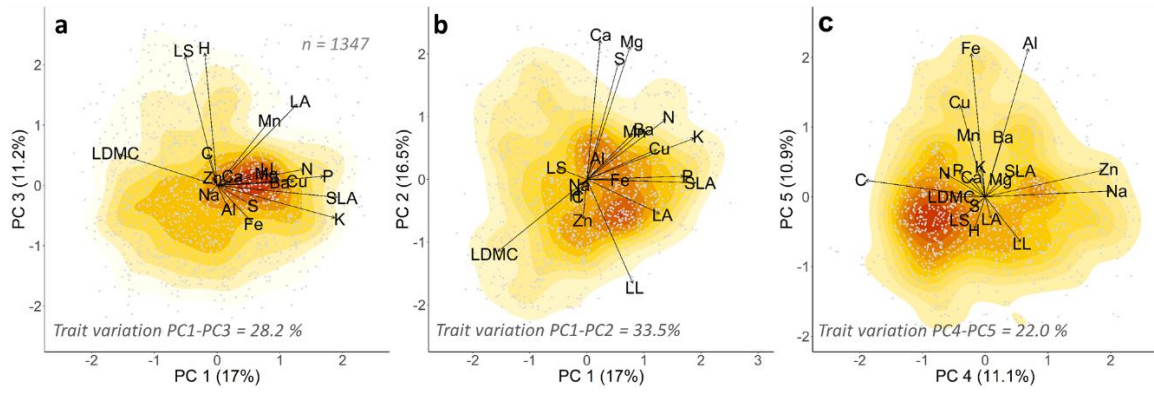
1183

1184

1185

1186

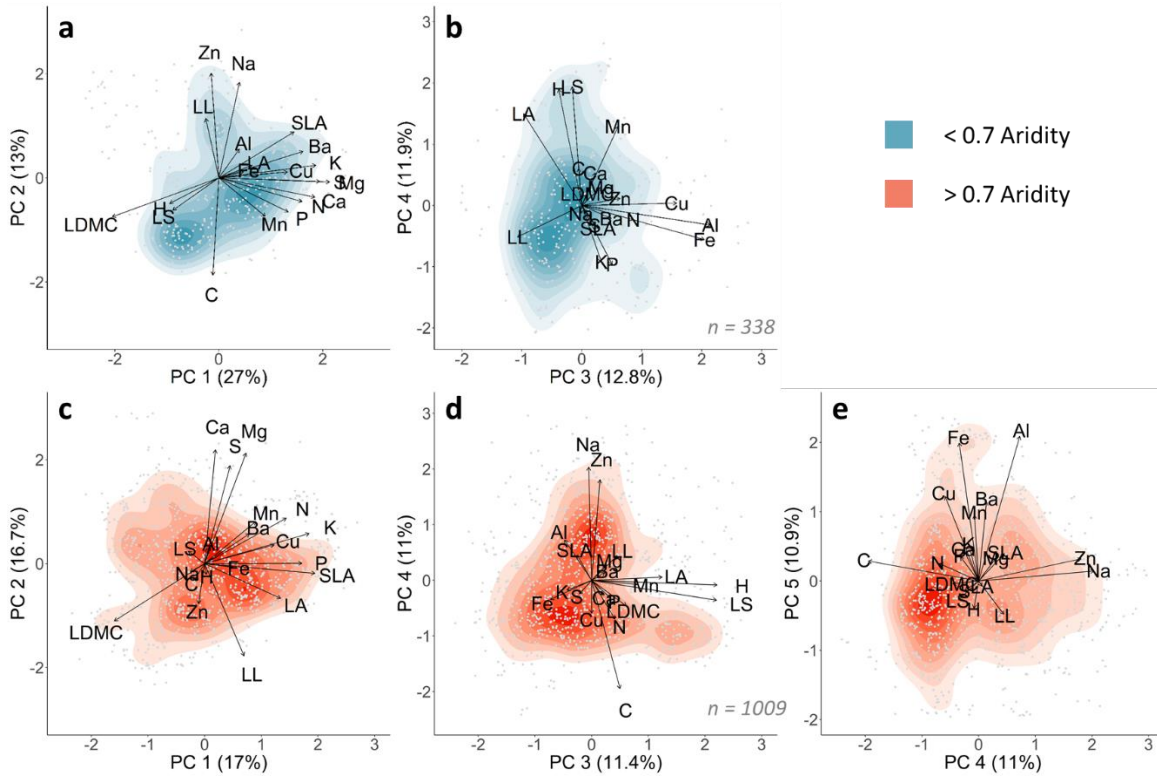
1187



1188

1189

1190 **Extended Data Figure 1.**



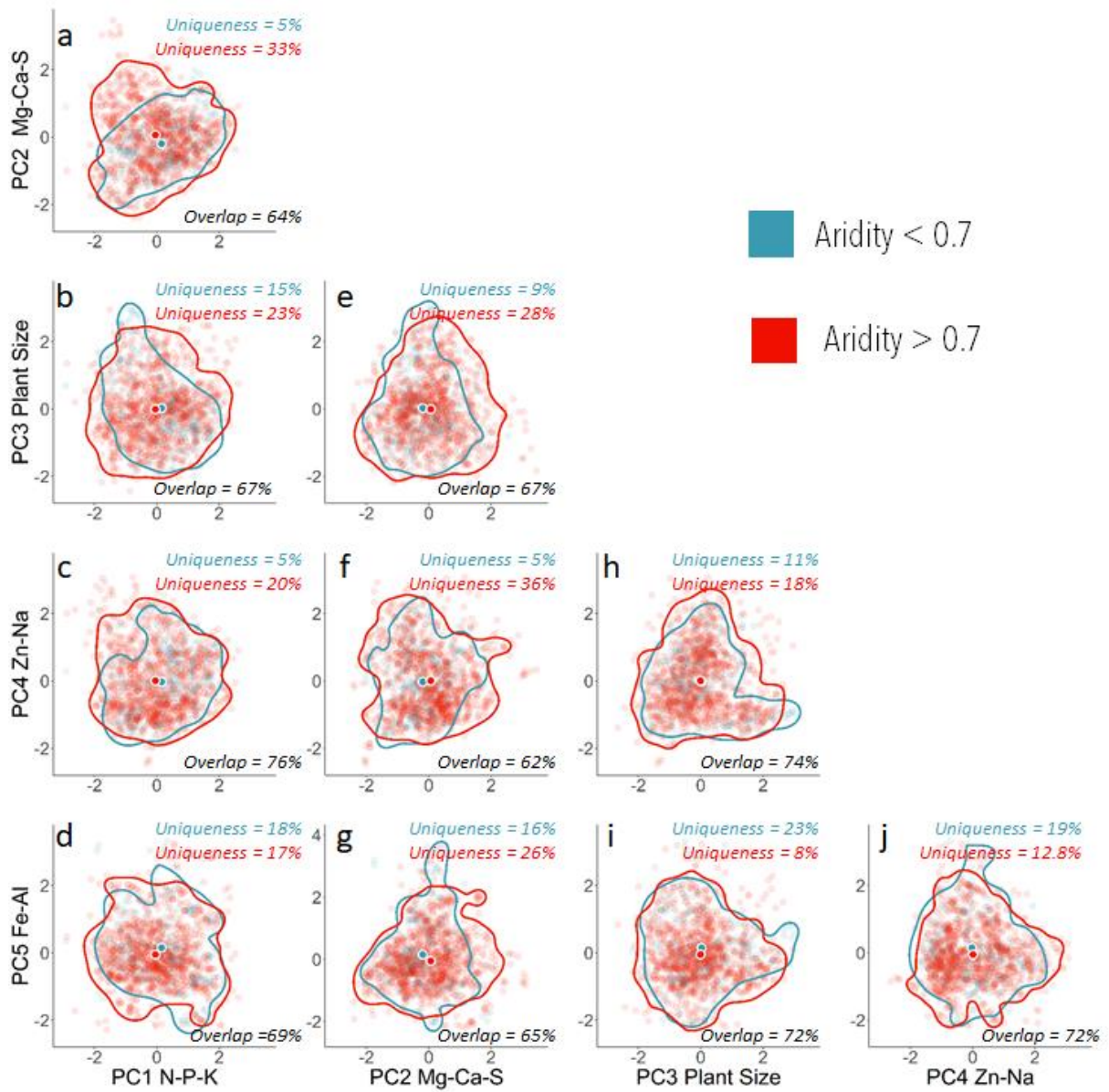
1191

1192

1193 **Extended Data Figure 2.**

1194

1195

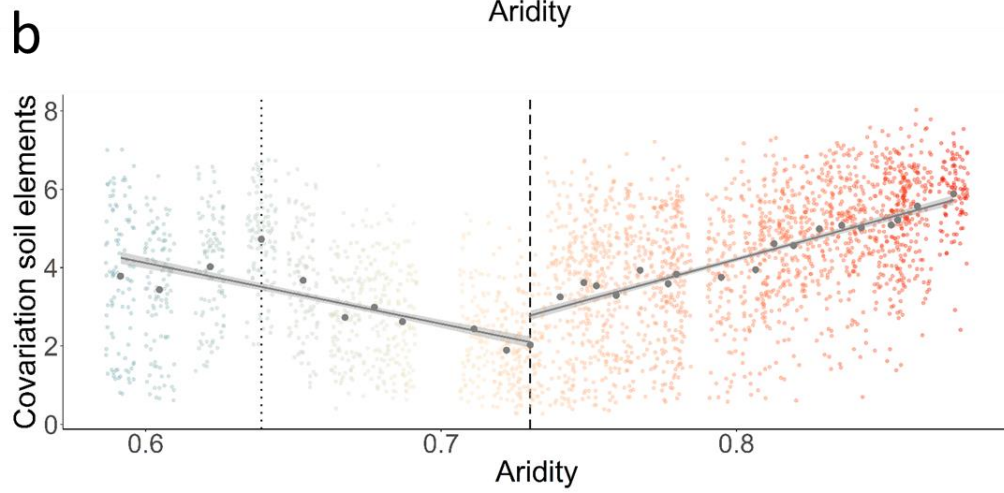
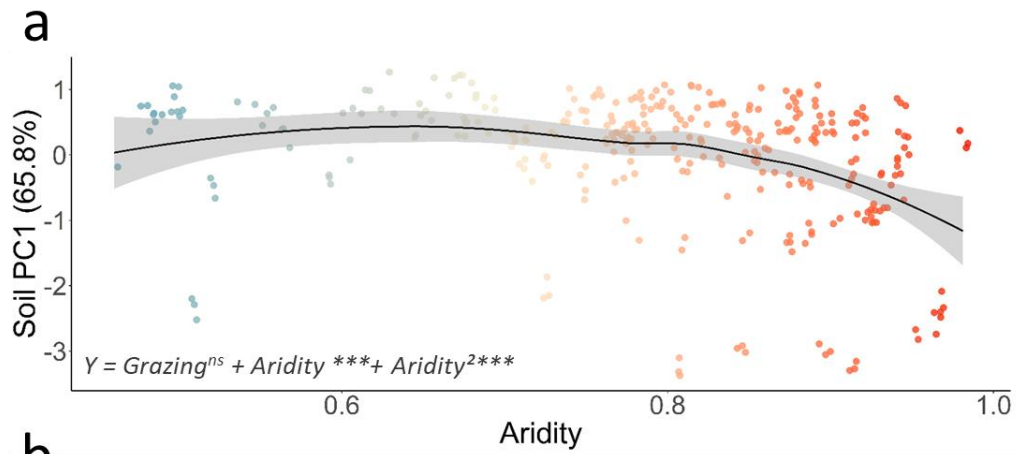


1199

1200

1201 **Extended Data Figure 4.**

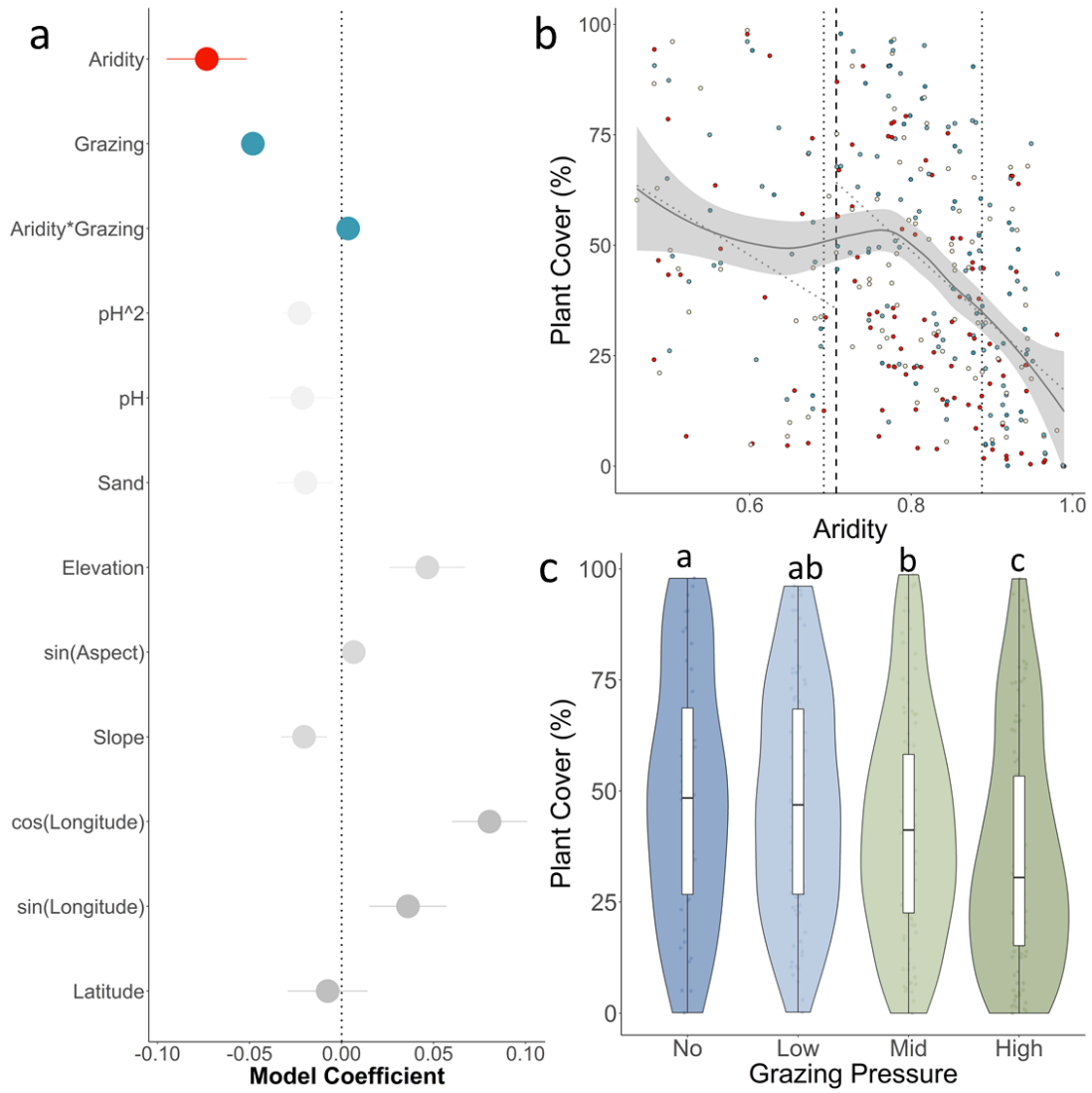
1202



1203

1204

1205 **Extended Data Figure 5.**



1206

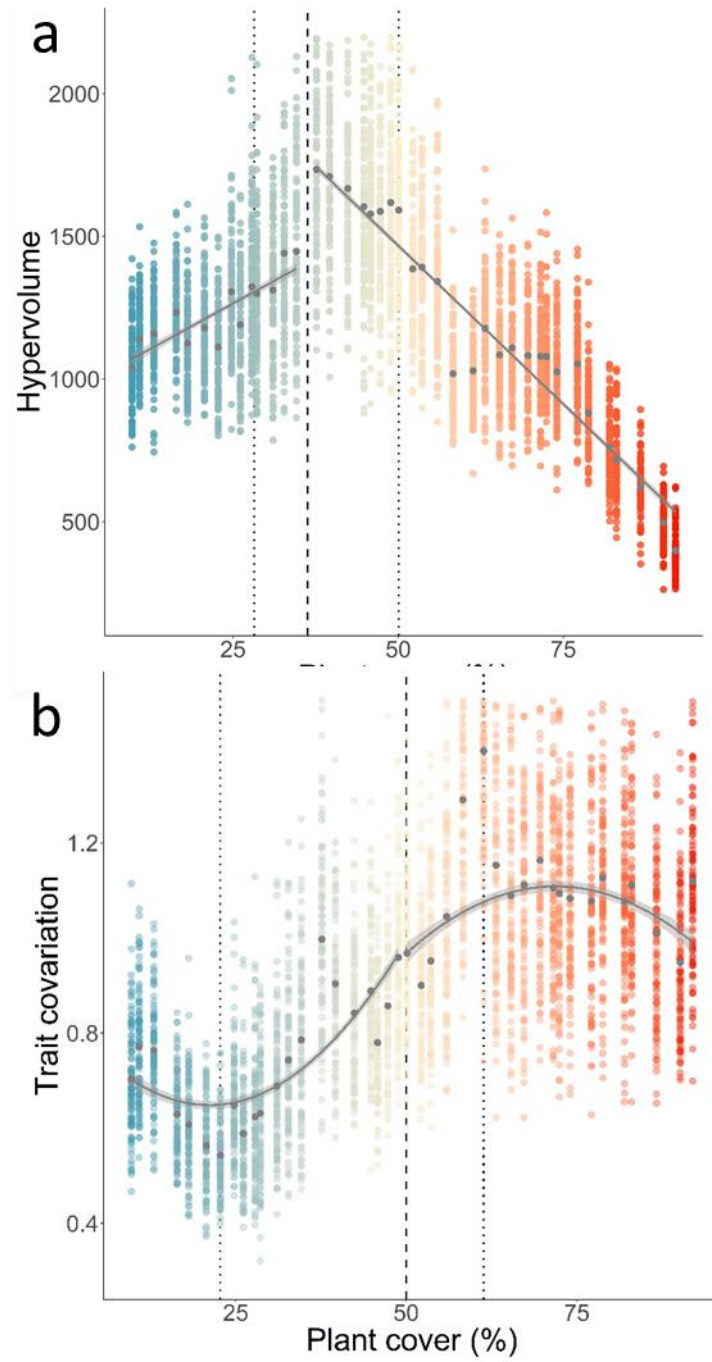
1207

1208 **Extended Data Figure 6.**

1209

1210

1211



1212

1213 **Extended Data Figure 7.**

1214